UCSF
UC San Francisco Electronic Theses and Dissertations

Title
Cadherin-13 maintains dendritic spine anatomy in the superior colliculus

Permalink
https://escholarship.org/uc/item/0cw6f8sh

Author
Matcham, Angela Cao

Publication Date
2022

Peer reviewed|Thesis/dissertation

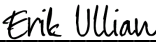Cadherin-13 maintains dendritic spine anatomy in the superior colliculus.

by
Angela Matcham

DISSERTATION
Submitted in partial satisfaction of the requirements for degree of
DOCTOR OF PHILOSOPHY

in

Neuroscience

in the

GRADUATE DIVISION
of the
UNIVERSITY OF CALIFORNIA, SAN FRANCISCO

Approved:

DocuSigned by:

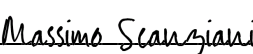*Erik Ullian*

1ACF3D77A55F4F0...

Erik Ullian
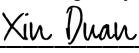
Chair

DocuSigned by:

Mercedes Paredes

DocuSigned by406...

Mercedes Paredes

Massimo Scanziani

DocuSigned by472...

Massimo Scanziani

Xin Duan

84E0C9F142DB4D5...

Xin Duan

Committee Members

DEDICATION

To my parents and grandparents

I cannot express in words how much your love and support has made me who I am,
but I have this work and a piece of fancy paper to show you.

~

语言无法描述你的爱与支持如何成就了现在的我，
但是希望这些成果可以帮我表达对你的谢意

CONTRIBUTIONS

The work presented in Chapter 2 of this dissertation has been prepared in the following manuscript:

Matcham A.C., Tsai N., Toma K., Sze C. Stewart I., Duan X. Cadherin-13 is Necessary for Trans-neuronal Dendritic Spine Maintenance in Superior Collicular Wide Field Cells. *In preparation.*

As the primary author, Angela Matcham, contributed the majority of the work in this manuscript as well as all aspects of Chapter 1 and Chapter 3 of this thesis unless otherwise directly stated.

Cadherin-13 maintains dendritic spine anatomy in the superior colliculus
Angela Cao Matcham

ABSTRACT

Understanding the molecular agents that direct and maintain synaptic connectivity and structure in the central nervous system (CNS) is critical in addressing many neurocognitive disorders. Mutations in cell adhesion proteins (Cadherins) that direct cell-type specific connectivity have been associated with autism, bipolar disorder and schizophrenia. The retinal-tectal projection, with its mutual laminar organization, provides a unique model system to identify cell type-specific cadherin expression and interrogate its mechanism. The central goal of this thesis is to identify candidate cadherins associated with restricted populations in the superior colliculus (SC) and to determine their role in directing circuit formation with retinal ganglion cell projections. In this study, Cadherin 13 is identified as a candidate cell adhesion protein in SC wide field cells. Cdh13 is a homophilic type 2 cadherin whose mutation is associated with ADHD, bipolar disorder, depression, autism and schizophrenia in human GWAS studies. In the CNS, Cdh13 has been shown to be involved in axon targeting and synapse regulation. This thesis explores the role of Cdh13 in cell type-specific pathway maintenance between the retina and wide field cells. *Chapter 1* describes new and necessary methods for consistent laminar and transsynaptic analysis that were developed during this research and can be expanded to further experiments and regions. *Chapter 2* explores Cdh13's expression patterns in conjunction with its temporal and spatial necessity in connectivity structures between the retina and SC. *Chapter 3* presents preliminary results further interrogating Cdh13's mechanisms in retinal-tectal connectivity. The culmination of these chapters not only detail cadherin 13's role in cell-type specific interactions between the retina and the SC, but also build upon established institutions to provide improved methods and updated information for future studies.

TABLE OF CONTENTS

LIST OF FIGURES

CHAPTER 1:

NOVEL METHODS FOR RETINAL-TECTAL LAMINAR ANALYSIS

INTRODUCTION:

The superior colliculus (SC) is a highly laminated structure, with both its inputs and resident cells organized in layers with specific morphologies and functionalities. The most superficial layers (sSC) are considered to be the retinorecipient layers that receive direct input from the retina and are responsive to visual stimuli. This area includes the stratus griseum superficiale (SGS) and the stratum opticum (SO). The retinal inputs into the sSC are laminarly segregated. For example, alpha retinal ganglion cell (aRGC) axons can be visualized by KCNG-Cre and terminate in the upper to mid SO (Fig. 1.1G) (Dhande & Huberman, 2014; Huberman et al., 2008). On-Off direction-selective RGC (ooDSGC) axons labeled by CART-CRE, on the other hand, terminate exclusively in the SGS (Fig. 1.1H) (Kay et al., 2011). There is also a functional organization in RGC axon segregation by layer (Dhande & Huberman, 2014). Motion-selective RGCs terminate their axons in the superficial layers of the sSC. Contrast- and center surround-detecting RGCs terminate in the deeper sSC layers. Accordingly, ooDSGCs, as the name suggests, respond to direction selective moving stimuli and their axons terminate in the upper SGS (Fig 1.1H). aRGCs, on the other hand, are not selective for motion and have SO terminating axons (Fig. 1.1G) (Dhande & Huberman, 2014).

Neurons in the SC are also laminarly segregated by both anatomy and function. Gale and Murphy 2014 identified 4 predominant morphological cell types in the sSC: stellate, horizontal, narrow field, and wide field cells. Stellate cells have small cell bodies with a small, complex, dendritic field and can be labeled by Rorb-Cre mice. They are found predominantly in the SGS and have small receptive fields that are not sensitive to motion. Horizontal cells are labeled by Gad2-Cre mice and have large receptive fields with no motion sensitivity. Narrow field cells are vertical oriented cells with narrow

dendritic fields labeled by GFP-KH288-Cre. These cells reside in the mid sSC on the border between the SGS and SO. They have small receptive fields and do not respond to moving visual stimuli. Wide field cells, labeled by NTSR1-GN209-Cre mice, have large cell bodies that sit low in the SO with large complex dendrites that extend to the surface of the SGS. They have large receptive fields and are responsive to small low moving stimuli.

The central goal of our lab is to associate molecular expression with morphological cell types for the purpose to identifying circuit directing actors. The goal of my thesis is to identify candidate cell-adhesion proteins (cadherins) and to understand their role in directing the cell types specific wiring. To accomplish this goal, a consistent laminar analysis protocol is necessary. In previous sSC studies (Huberman et al., 2008; Kay et al., 2011; Kim et al., 2010; Tsai et al., 2022; Zhang et al., 2012), laminar analysis is both necessary yet relatively arbitrary. The conventional analysis protocol involves comparing relative depth from the surface of the SC (Fig 1.1D). In many cases, laminar boundaries are then approximated with little to no reported methods. Although great care is taken to ensure consistent tissue collection methods and regional consistency, variability is unavoidable. Because of this, it was necessary to develop a new analysis method that significantly reduces this variability.

The SC is a large structure that spans approximately 2000um x 2000um in the adult mouse, with varying layer thicknesses at each coordinate. Within a single coronal slice, layer thicknesses vary greatly between medial and lateral areas (Fig 1.1B). The relative depth of the fluorescence (Fig 1.1D) varies wildly between medial and lateral locations in the same coronal slice, even though their laminar location remains consistent (Fig 1.1E). Even when exact, consistent coordinates for comparison are attempted, large differences between general morphology and layer thicknesses can be observed within the same mouse. Even worse, variations between mice, even in the tissue preparation or slice orientation, can cause large differences between samples. A salient example of this can be observed in

layer differences in the SC between two prominent mouse brain atlases, "Allen Mouse Brain Atlas" and "The Mouse Brain in Stereotaxic Coordinates" by Keith B.J. Franklin and George Paxinos.

These variations make it difficult to appropriately analyze laminar location of RGC axons and SC cells, especially under conditions of sparse labeling. Even if exact layer replication between samples for a specific coordinate is achieved, the data would then be severely limited due to its anatomical restriction to a single 40um region. The conventional analysis method gives a crude approximation of laminar locations of the SC and the quantitative outputs are severely compromised by it.

RESULTS

Due to the limitations of conventional methods for sSC laminar analyses, discussed above, it was necessary to develop a new method to detect variations in layer thickness. This was achieved by creating an automated analysis protocol that relies on immunohistochemically visualized laminar boundaries. This provides the method to standardize sSC analyses regardless of variations in thicknesses. The boundary between the SGS and the SO can be visualized by staining for myelin-based protein, MBP (Fig. 1.1A, red). The lower SO boundary can be visualized by the upper boundary of VachT staining while the lower boundary labels the lower SGI boundary (Fig 1.1A, blue). These immunohistochemical stains were previously described by (Byun et al., 2016). In this study, their use in laminar fluorescence detection and normalization using a semi-automated program allows for accurate laminar visualization regardless of animal variation, tissue preparation, or location within the SC.

Specifically, a semi-automated protocol was developed to use these boundaries and normalize the target florescence distribution by layer, allowing for consistent resident layer designation and subsequent fair comparison across regions and samples. The automated program requires two inputs: (1) the isolated boundaries of the sample defined by immunohistochemistry, and (2) the confocal image of the target fluorescence in the same sample. 200um bins are taken at perpendicular intersections from the surface of the SC through to the lower boundary of the SGI. This allows for analysis regardless of the surface curvature of the region. The relative target fluorescence is quantified from the SC surface to the lower boundary of the SGI. The fluorescence is then normalized by their relative pixel intensity and their laminar location is normalized based on their relative location to the laminar boundaries (Fig. 1F-H). This method allows for the collection and comparison of not only the entire medial-lateral length of a single coronal section, but it also allows for the comparison between different areas of the SC and between animals.

The protocol was validated on established mouse lines with known RGC axonal lamination including wild-type pan-RGC lamination, alpha-RGC lamination, and on-off direction-selective RGC lamination. First, the protocol's ability to quantify pan-RGC axons was confirmed by analyzing CTB-labeled axons (Fig 1.1F). The axons were confirmed to be restricted to the sSC with the highest density in the SGS and a gradual decline in the lower SO. aRGC axons labeled by KCNG-Cre are shown to be restricted to the SO as previously described in the literature (Duan et al., 2015)(Figure 1.1G). ooDSGC axons labeled by CART-Cre are also confirmed to be concentrated in the SGS with this method (Fig 1.1H).

Although the laminar boundary method confirms previous descriptions of axonal lamination, there are some details that are only resolved using this process. For example, although a majority of aRGC axons terminate in the SO, a few axons extend into the SGS. Conversely, a majority of ooDSGC axons terminate in the SGS, but a few axons extend into the SO. The previous relative depth analysis method would not have been able to resolve the minor nuances in RGC axon restriction. Therefore, in the case of detecting changes in lamination due to experimental manipulation, the laminar boundary method will be able to detect more acute changes than when observing relative depth. The laminar boundary analysis not only allows for a fair comparison of laminar distribution across samples, but it also provides information otherwise undetectable by previous methods.
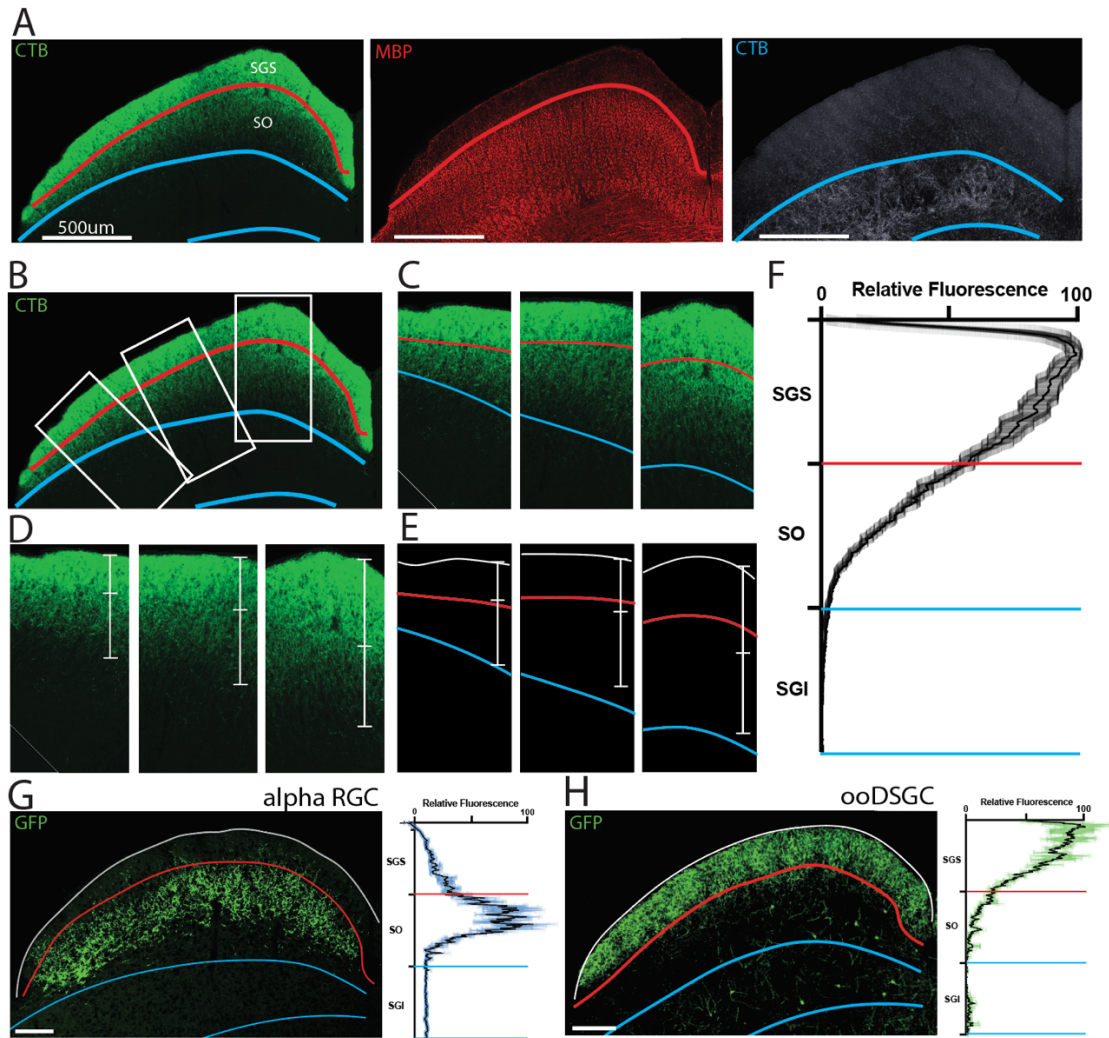
Figure 1.1 Novel method for SC laminar analysis allows for more accurate quantification and analysis.

(A) Confocal images of CTB-labeled RGC axons (green, left) with MBP (red, middle) and VachT (blue, right) immunohistochemical stains to label the lower SGS and SO boundaries. The colors of the stains (red = MBP and blue = VAchT) will mark the location the associated laminar boundary (red = lower SGS, blue = lower SO) for the duration of this study.

(B) Three rectangular segments perpendicular from the sample shown in (A) are isolated and compared in (C).

(C) Comparison of segments from the same coronal section shown in (A) and (B) from lateral (left) to medial (right).

(D) Demonstration of the large range of results observed if relative depth is used to analyze laminar location. The white vertical bar represents the CTB positive area with the center white horizontal notch representing the transition between the high-density and low-density areas.

(E) The white bars representing the CTB lamination from (D) is compared to the immunohistochemically defined laminar boundaries.

(F) Laminar quantification analysis method of pan-RGC axons labeled by CTB. (Mean ± SEM)

(G) Confocal image of alpha RGC axons innervating the SC labeled by AAV2-DOO-GFP (left). Quantification of normalized laminar distribution of relative fluorescence of aRGC axons in the SC (right).

(H) Confocal image of On-Off direction-selective RGC axons innervating the SC labeled by AAV2-DIO-GFP (left). Quantification of normalized laminar distribution of relative fluorescence of ooDSGC axons in the SC (right).

DISCUSSION

This new laminar boundary method for SC layer analysis discussed in this section overcomes the limitations of previous approaches. It provides consistent standardization of laminar location across SC regions. The current standard SC laminar analysis method using relative depth analysis omits critical details about laminar organization. Between adjacent SC locations, the relative depth of the pan-RGC axons will vary widely (Fig 1.1D) but they will be consistent in its relation to its layer location (Fig 1.1E). Previous studies were therefore restricted to comparing only one SC location, typically with a exemplary image rather than a multi-sample quantification. The laminar boundary method accounts for changes in laminar thickness to allow for the quantitative analysis of samples from different SC regions and between animals.

This method overcomes another disadvantage of relative depth analyses. Since relative depth analysis cannot to determine the true locations of the laminar boundaries, populations along boundary boarders can be miscategorized. This method allows for accurate detection of neurons beyond the sSC in the SGI, such as Etv1-cells that have been previously mis-categorized as SO neurons.

The following section describes several WGA-tracing experiments that also benefit from the precision and depth resolution of this method. WGA-mCherry labeled cells are detected just below the SO boundary in the SGI, indicating that there are retinal-recipient cells outside of the classic retinorecipient layers. These cells are very close to the SGI/SO boundary and would be easily overlooked by conventional analysis methods. Using the laminar boundary analyses, these cells can be properly defined. The laminar boundary method allows for greater resolution in SC studies to both define its composition as well as a tool for experimental manipulations in the area. Not only that, but the analysis method code is also not SC dependent, and therefore could be further applied to other laminar CNS regions with immunohistochemically defined layers, such as the cortex.

CHAPTER 1.2: METTHODS OF WHEAT GERM AGGLUTININ TRANSYNAPTIC TRANSFER DETECTION AND ANALYSIS

INTRODUCTION

Wheat Germ Agglutinin (WGA) is a lectin produced by plants to protect themselves from predators and parasites. WGA binds to the carbohydrates of glycoproteins on cellular membranes. As a scientific tool, WGA has been used in cancer therapy (Ryva et al., 2019) and as a neuronal transsynaptic tracing tool (Basbaum & Menetrey, 1987). As a transsynaptic tracing tool, it has been shown to be transported in both the anterograde and retrograde directions (Horowitz et al., 1999; Yoshihara et al., 1999), allowing for a variety of technical applications. Fluorescent or HRP conjugated WGA protein has been extensively studied and utilized in previous literature to trace neuronal connectivity in mouse and primate systems.

A disadvantage of previous WGA methods is the inability to specify the starting population within the injection region. This prevents accurate identification of the pre- and post-synaptic populations, making it difficult to use this system to map cell type-specific circuits. To address this issue, our lab developed a virally mediated, Cre-dependent, WGA protein. This allows for specific targeting of a starting cell population based on positive Cre-expression. And to allow for visualization of WGA transsynaptic transfer, a fluorescent protein marker (mCherry) was fused to the WGA.

The accuracy and efficiency of our AAV2-DIO-WGA-mCherry in monosynaptic transsynaptic transfer was confirmed via electrophysiology (Tsai et al., 2022). The central goal of the lab is to identify molecules responsible for directing cell type-specific wiring between the retina and the SC. Using virally mediated WGA as a transsynaptic tracer from the retina, we can identify candidate molecules in post-synaptic populations in the SC. An accurate and efficient protocol for WGA-positive neuron visualization and identification is necessary for the effectiveness of our novel transsynaptic tool. This section describes a variety of analysis tools and methods developed to address this goal.

RESULTS

WGA is a lectin that prefers to reside on the cell membrane or in lysosomes in the cytoplasm. When coupled to the mCherry fluorescent marker, the resulting fusion molecule tends to form puncta throughout the cell, including the axons and dendrites. This punctation is evident in both the starting population and the post-synaptic population. Because of this sea of dotted signals, the post-synaptic cells in the SC become difficult to identify as positive or negative for transsynaptic labeling.

The first method investigated in this study for visualizing post-synaptic cell bodies was to first label cells with DAPI or NeuN to visualize all cells or neurons, respectively. Then identification of mCherry+ co-expression via pixel overlap with DAPI or NeuN in the confocal image would allow for the identification of retinorecipient cells. By labeling all cells, this method would allow for identification of the total population size to determine the proportion of SC cells that receive direct retinal input. Unfortunately, given the nature of WGA-mCherry forming clouds of mCherry punctate in the cytoplasm and cell membrane, direct co-expression within the nucleus does not capture the whole WGA(+) post-synaptic population. Therefore, automated pixel masking analysis to determine co-expression is not optimal. Two visualization methods were therefore developed to address this issue.
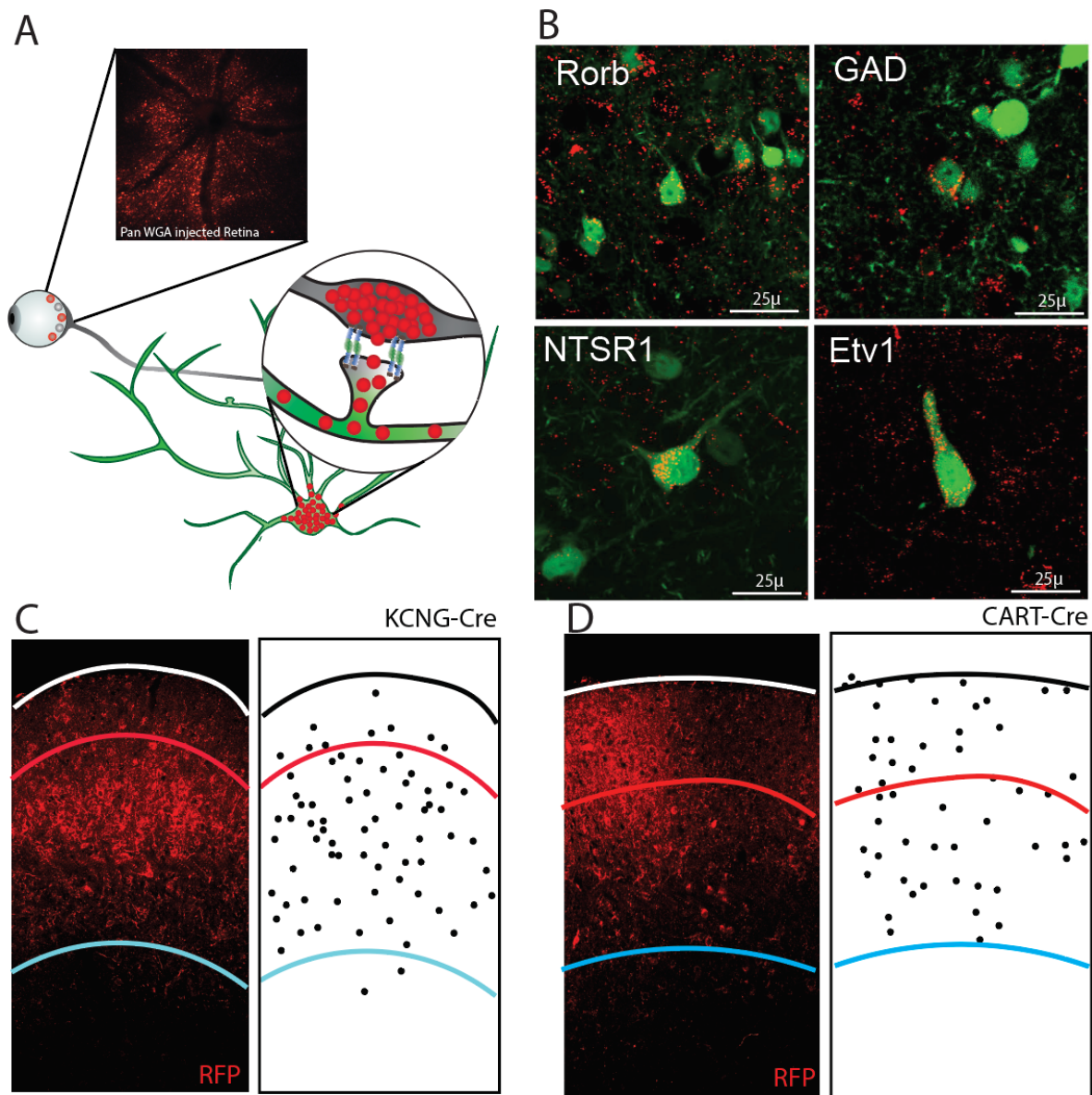
Figure 1.2 Analysis methods for WGA-mCherry transsynaptic transfer identification
(A) Schematic of WGA-mCherry transfer from infected RGC starting population in the eye to postsynaptic populations in the retina.
(B) Example stellate, horizonal, wide-field, and Etv1 neurons that receive direct retina input.
(C) Confocal image of WGA-mCherry labeled post-synaptic population of KCNG-Cre labeled aRGCs (left). The infected cell bodies are notated by individual uniform circles in their respective position on the right.
(D) Confocal image of WGA-mCherry labeled post-synaptic population of CART-Cre labeled ooDSGCs (left). The infected cell bodies are notated by individual uniform circles in their respective position on the right.

Pre-identification of SC cell type

Identification and quantification of retinorecipient cells first requires a cytoplasmic or membrane bound label in the target SC population. Having this in the post-synaptic population allowed for WGA-mCherry overlap with the post-synaptic cell label. Automated detection processes were then used to systematically and efficiently detect mCherry(+) and mCherry (-) in the target population.

This method can determine the percentage of established sSC populations that receive direct retinal input. Using transgenic mouse lines to label specific SC populations, the percentage of stellate (Rorb-Cre), horizontal (GAD2-Cre), wide-field (NTSR1-GN209-Cre), and Etv1 cells (Etv1-CreER) that are directly retinal-recipient was determined. A pan-neuronal WGA-mCherry (AAV2-WGA-mCherry) is injected into adult mouse retinas of each of these mouse lines. Of the target SC cell populations, 89.13%± 5.37% of stellate (n = 540 cells), 82.95%±11.10% of horizontal (n = 228 cells), 85.31%±7.00% of wide field (n = 125 cells), and 4% of Etv1 cells (n = 50 cells) were WGA-mcherry positive . It is interesting to note that stellate, horizontal, and wide-field cells reside in the sSC, while Etv1 cells reside in the upper SGI. Therefore, it is not surprising that a majority of the sSC residing cells receive direct retinal input while Etv1 cells do not, since sSC is considered the retinorecipient layers. However, it is a novel observation that some Etv1 neurons do receive direct retinal input (Fig. 2B), given their location outside of the sSC. These neurons have large dendritic arbors that extend into the sSC, therefore it is not surprising that they could receive direct retinal input. However, given that a majority of this population sends dendrites into the sSC, it is then, surprising that a larger percentage of this population does not receive direct input.

The central goal of the lab is to identify the molecules that direct partner choices between the retina and the SC. An important part of this process is determining which SC cells receive direct retinal input. Through the use of the methods discussed, Etv1 cells outside of the sSC in the SGI are

discovered to receive direct retinal input. It is also notable that the non-retinorecipient Etv1 cells also has dendrites that co-laminate with RGC axons, but do not form synaptic connections. The identification of this population allows for future studies looking at synaptic partner choice. Etv1 cells can be used as a negative control or a vehicle to demonstrate how the misexpression of candidate proteins can direct connectivity with specific RGC inputs.

Laminar Quantification

WGA-mCherry(+) cell distribution can be informative and detected without a post-synaptic cell marker. This allows for cell type-specific starting population targeting in the retina using a Cre-driver line. Although this also allows for a greater range or presynaptic specificity, this method is not able to determine the cell type of the post-synaptic cell. It is also unable to determine the number of negative cells in the population. Nevertheless, differences in recipient cell lamination are informative since SC cell types are laminarly organized.

Using this method, the post-synaptic populations of aRGC and ooDSGCs were compared. AAV2-DIO-WGA-mCherry was injected into adult KCNG-Cre and Cart-Cre eyes to label aRGCs and ooDSRGCs, respectively. Two weeks later, SC samples were fixed and collected. In each condition, mCherry(+) cells were identified and the cell body position recorded using equal sized polygons. The positive cells were identified manually in ImageJ by either observing the confocal image stack in 3-dimensions or scrolling through the z-stack to resolve a punctated shell. The distribution of the post-synaptic population could then be quantified laminarly using the previously discussed laminar quantification method.

The method of identifying each positive cell in this manner serves two purposes. First, for laminar analysis, fluorescence from axons and dendrites will be omitted. Therefore, the data will not be biased by neurite fluorescence. For example, WF cells in the SO would also have positive signals

in the dendrites that extend to the SGS, thereby skewing the data towards the SGS. RGC axon terminations would also skew the data (Fig 1.2C). Secondly, there are large differences in cell body size. A large cell would contribute greater relative fluorescence than a smaller cell, thereby skewing the data towards locations with larger cells. This method normalizes for cell size, so each cell is equally represented in the distribution data (Fig. 1.2C, D right).

Using this method, the aRGC and ooDSGC post-synaptic population distributions can be appropriately compared. The aRGC projectome includes cells in the lower SGS, throughout the SO, and a few beyond in the retino-recipient sSC in the SGI (Figure1. 2C right). The ooDSGC projectome, on the other hand, resides in equal distribution from the surface of the SC through the SGS and SO. No SGI neurons were innervated by ooDSGCs. aRGCs therefore seem to innervate sSC neurons that are on average in deeper layers than those innervated by ooDSGCs, echoing their axonal lamination differences. Because of the laminar segregation of neuronal populations in the SC, a laminar difference in post-synaptic population likely translates to a difference in the post-synaptic cell types. This question was further explored in (Tsai et al., 2022) where we used single cell RNA-sequencing of WGA-labeled sSC neurons to compare projectomes of different RGC subtypes.

Although the aRGC and ooDSGC projectomes mirror their laminar differences, in both cases the distribution of the postsynaptic population is greater than that of their innervating axons. Although aRGCs axons are restricted to the upper SO, the post-synaptic neurons are in the SGS, lower SO, and SGI (Fig 1.1G, Fig 1.2C). Likewise, the ooDSGC post-synaptic population includes many cells well below ooDSGC axon terminations. This data collected using these methods expand on our previous understanding of retinal-tectal connectivity, demonstrating the wide distribution of retinal input despite restricted axon innervation.

DISCUSSION

WGA has long been a useful tool for transsynaptic research. The development of a virally mediated Cre-dependent WGA with a fluorescent tag allows for rapid expansion of WGA-based applications. This is only possible with a reliable analysis method for WGA-mCherry detection for accurate identification of positive vs negative post-synaptic transfer. Two methods were developed for WGA-mCherry transfer analysis that are effective in comparing retinal projections to the SC: SC population labeling, and manual 3D identification.

Although SC population labeling can help determine the percentage of stellate, horizonal, WF, and Etv1 populations that receive retinal input, the method has its disadvantages. Labeling these populations require the use of Cre-driver lines. Therefore, genetic access to RGC subpopulations was not possible. This method is unable to determine the connectivity between RGC subtypes with each of these SC populations. On the other hand, manual 3D identification of WGA-mCherry positive cell bodies allows for starting population specification but does not allow for identification of the post-synaptic cell type. Neither method is applicable for all AAV-WGA experiments, but their use can be applied to a variety of future projects as new technologies develop.

The lab is currently researching methods to bridge this technological gap. Efforts have been made to isolate WGA-mCherry positive cells via flow-cytometry. These cells then undergo single-cell RNA sequencing to determine the cell types in the post-synaptic populations. This method can be implemented in RGC-Cre driver lines to allow for both the presynaptic starting population specification and post-synaptic cell type identification (Tsai et al., 2022). There are also efforts in the lab to create cell-type targeting mini-promoters. These mini promoters would be designed to be transcribed only in specific cell types. This would allow for RGC starting population-specific targeting without the use of a Cre-driver line. This in turn, would allow for post-synaptic population identification using Cre-driver lines without losing starting cell specificity.

SUMMARY

Appropriate data analysis protocols are the hallmark of reproducible, accurate science. Development and optimization of these methods are the foundation of any project. The improved methods described in Chapter 1 address issues with current superior collicular laminar analysis methods (Chapter 1.1) and optimize methods for our novel transsynaptic tracer tools (Chapter 1.2). These methods allow a more precise means of defining the regions and identifying the location of different cell types within the SC. Having established these methods, the project research then focused on defining the role of Cadherin 13 in protein mechanisms that connect the different cell types within the SC, described in Chapter 2. The methods described here in Chapter 1 are also applicable for future studies, such as some described in Chapter 3.

CHAPTER 2:

CADHERIN 13 MAINTAINS SPINE DENDRITIC MORPHOLOGY IN SUPERIOR

COLLICULAR WIDE FIELD CELLS.

INTRODUCTION

The ability to integrate visual stimuli relies on neuronal pathways from retinal ganglion cells to the brain. These parallel projections require protein mechanisms to find and maintain contact with their correct post-synaptic partners (Sanes & Yamagata, 2009; Yamagata et al., 2003; Yogev & Shen, 2014). A family of calcium-dependent cell adhesion molecules (Hirano & Takeichi, 2012), cadherins, have been shown to direct this process in various CNS circuits. Cadherins localize in synaptic junctions (Benson & Tanaka, 1998; Fannon & Colman, 1996; Huntley & Benson, 1999; Uchida et al., 1996; Yamagata et al., 1995) and are necessary in various phases of LTP (Bozdagi et al., 2000; Manabe et al., 2000; Tanaka et al., 2000; Tang et al., 1998) and in directing circuit specific connectivity (Duan et al., 2014; Duan et al., 2018). In the retina, Cdh8 and Cdh9 were shown to direct bipolar cell axonal targeting and synaptic specificity in both their wild type and misexpressed conditions (Duan et al., 2014). Further, a combination of Cdh6, Cdh9, and Cdh10 were shown to direct direction-selective visual input to a specific retinal ganglion cell (RGC) subtype (Duan et al., 2018). These RGCs then relay different aspects of the visual world to the brain via a critical visual processing center, receiving direct retinal input, known as the superior colliculus (SC). This study aims to understand the role cadherin expression plays in directing the wiring of parallel informational channels in the SC. Cadherin expression is surveyed in the SC then anatomical changes are observed under targeted cadherin manipulations.

The superior colliculus' neuronal populations and its inputs are laminarly organized. Functional processes within the SC are laminarly organized as well with the most superficial layers (sSC) considered to be the retinorecipient layers. They receive direct input from the retina and are responsive to visual stimuli. This area includes the stratus griseum superficiale (SGS) and the stratum opticum (SO). Previous studies have characterized the cell types in the sSC by their molecular expression (Byun et al., 2016) or their morphology and functional properties (Gale & Murphy, 2014).

As described in the introduction to Chapter 1, Gale and Murphy identified 4 predominant cell types in the SC based on their anatomy, physiology, and visual response preferences: stellate, horizontal, narrow field, and wide field cells. Using the transgenic lines to label these cell types, our lab aims to associate cell adhesion protein expression with these morphological cell types. In this study we aim to understand the role cadherins expression play in directing the wiring of parallel informational channels.

To identify candidate cadherins that direct specific retinal-tectal connectivity, cadherin expression patterns were surveyed using transgenic mouse line labeling (Chapter 2.1). This was then compared to established SC cell types (Gale & Murphy, 2014, 2018) using in situ hybridization. Through this process, cadherin-13 was observed in our studies to be uniquely enriched in wide field cells (WF) (Chapter 2.2). Cdh13 is a unique, type-II cadherin that is necessary for axonal targeting, synaptic targeting, and synaptic regulation in a cell type specific manner (Hering et al., 2003). It is a homophillically binding cadherin, coupled to a Glycosylphosphatidylinositol (GPI) moiety instead of an intracellular domain. GPI domains are typically found in association with lipid rafts, which have been shown to be necessary in dendritic spine anatomy, function, and maintenance (Ciatto et al., 2010; Kiser et al., 2019; Nguyen et al., 2020; Philippova et al., 2008; Rivero et al., 2015). Spines are the primary site of glutamatergic input that allow for the aggregation of necessary post-synaptic proteins and are therefore critical for appropriate transsynaptic communication. Cdh13's unique enrichment in WF cells, its GPI coupling, and its role in circuit regulation make it a prime candidate in RGC specific connectivity of WF cells.

To determine the role of Cdh13 in the connectivity between RGCs and WF cells, we observed the changes to dendritic spine populations under a variety of knock-out or knock-down conditions using both genetic mouse lines and viral delivery. When Cdh13 was endogenously knocked out, mature WF dendritic spines were significantly decreased, with a disproportionate loss in the apical

dendritic regions. This loss was similarly observed when Cdh13 was knocked down in the WF cells in adulthood. Because Cdh13 acts in a homophilic manner (Lehto & Sharom, 1998; Tanihara et al., 1994) we wanted to know what Cdh13-expressing inputs partner with WF cells apically and whether disrupting Cdh13 in these presynaptic populations would result in a similar spine reduction. We found that Cdh13-expressing RGC axons co-terminate with WF apical dendrites. Subsequently, Cdh13 knockdown in these RGCs locally decreased WF mature spine densities in their axonal termination zones. We conclude that trans-neuronal Cdh13 is necessary for the maintenance of mature dendritic spines in a cell type-specific manner. Since RGCs provide glutamatergic innervation and dendritic spines are the primary site of glutamatergic input in the CNS, a change in dendritic spine anatomy is likely to affect glutamatergic synaptic communication. In fact, reductions in spine number has been shown to negatively affect synaptic function and is a common feature of early neurodegenerative diseases such as Alzheimer's (Boros et al., 2019; Boros et al., 2017). Given this, the results indicate that Cdh13 is necessary in adult spine maintenance and that it is likely integral to maintaining communication between specific RGC populations and WF cells.
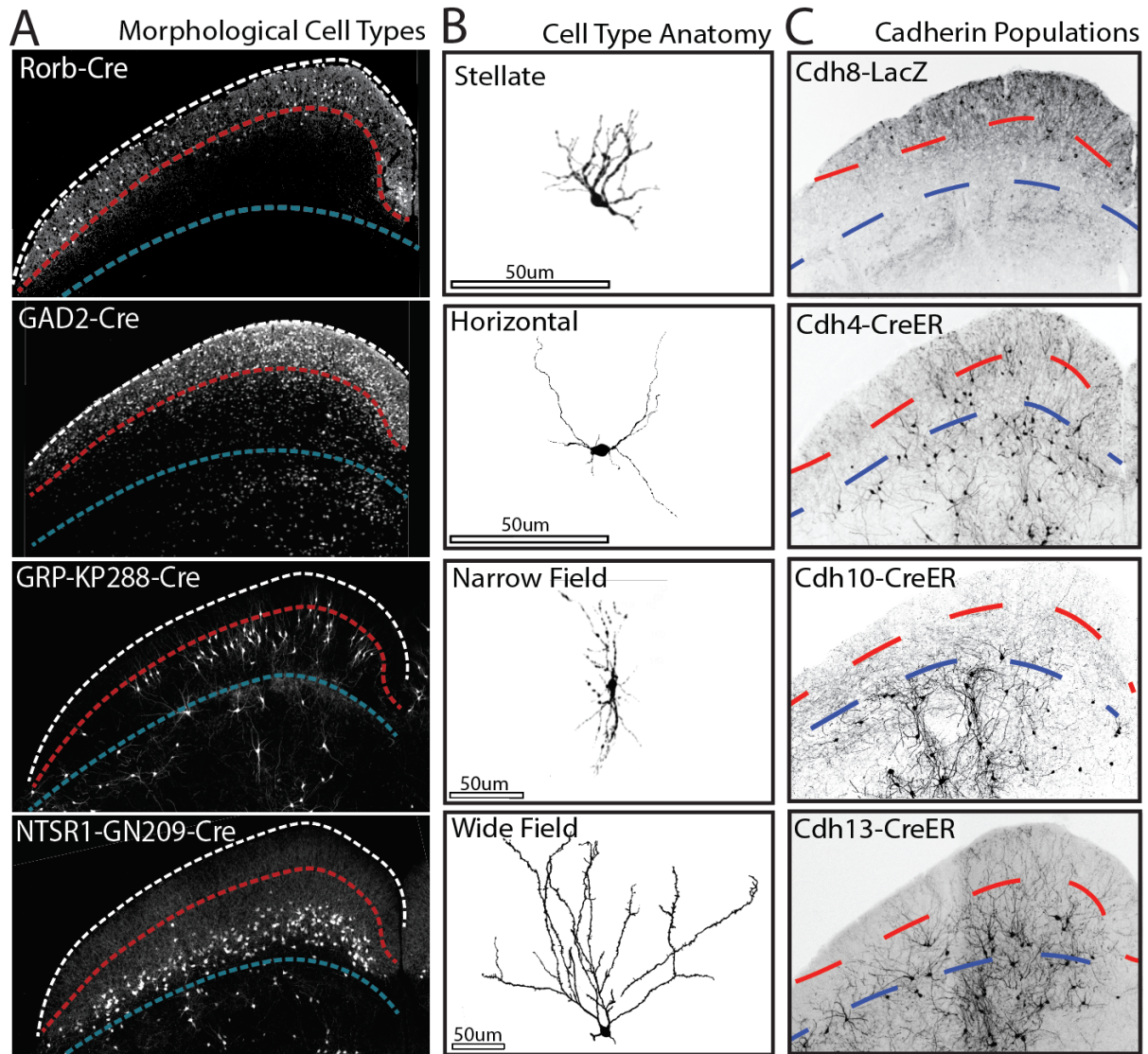
Figure 2.1. Genetic mouse lines can visualize anatomical and cadherin-expressing cells types in the SC.

(A) Confocal images of established morphological cell lines in the SC visualized using different Cre lines. Stellate cells are labeled by Rorb-Cre, horizontal cells are labeled by GAD2-Cre, narrow field cells are labeled by GRP-KP288-Cre, wide field cells are labeled by NTSR1-GN209-Cre. The laminar location of each population can then be compared using immunohistochemical methods previously defined (Fig. 1.1).

(B) Isolated neurons taken from confocal images of the mouse lines in (A). Neurons were isolated using ImageJ neurite tracer.

(C) Confocal images of cadherin expressing cells in the SC labeled by Cre-ER expressing mouse lines. Cdh8 is labeled by Cdh8-LacZ mouse line. The laminar location can then be compared.

RESULTS

Chapter 2.1: Cadherin-13 is uniquely enriched in WF Cells in the Superior Colliculus

To understand how cadherins direct retinal-tectal parallel projection wiring, it is important to know the expression patterns of these cadherins in the sSC. To visualize cadherin expression patterns, we stained for the mRNA of various cadherins in mouse sSC in comparison to established sSC cell types (Gale & Murphy, 2014, 2018). This not only helps us understand cadherin expression patterns in the sSC, but it also allows us to find candidate cadherin/SC population pairs in order to investigate the role of those cadherins in those cell populations. To standardize and visualize the laminar boundaries of the sSC, we stained for established molecular markers. Their laminar locations were compared to the laminar locations of these anatomically defined cell types (Fig 1.1, Fig. 2.1). As described in Chapter 1, the boundary between the SGS and SO is visualized by MBP staining and the lower SO boundary is visualized by VachT staining (Byun et al., 2016) (Fig 1.1). The established cell types: stellate, horizontal, narrow, and wide field, were visualized by transgenic mouse lines using Rorb-Cre, GAD2-Cre, GRP-KP288 -Cre, and NTSR1-GN209-CRE respectively (Gale & Murphy, 2014), mated to our lab's Cre-dependent YFP line, Thy1-STP-YFP, (Buffelli et al., 2003) (Fig 2.1A). Rorb-Cre stellate/horizontal cells were restricted to the SGS. GAD2-Cre horizontal cells resided in the SGS and upper SO. GRP-KP288-Cre narrow field cells resided along the SGS/SO boundary. NPNT1-GN209-Cre wide field cells have cell bodies in the lower SO with large, complex, dendritic arbors that reach to the upper SGS (Fig 2.1A bottom).

To visualize cadherin expression in the sSC, we surveyed cell labeling in cadherin-targeting transgenic mouse lines. We specifically assessed the expression pattern of Cdh4, Cdh8, Cdh10, and Cdh13 given their importance in cell type-specific connectivity in other systems (Fig 2.1C). Cadherin 4 is robustly expressed in both the retina and the superior colliculus and has been shown to be a necessary component of retinal ganglion cell development and RGC axonal projection and

arborization in the SC (Babb et al., 2005). Cadherin 13 is necessary for axonal targeting and synaptic functionality in the spinal cord, cortex, and cerebellum in a cell type specific manner (Kiser et al., 2019; Nguyen et al., 2020; Philippova et al., 2008; Rivero et al., 2015; Tantra et al., 2018). Of the assessed cadherins, Cadherin 13 has a notable laminar enrichment in what is predicted to be the lower SO (Fig 2.1C bottom).

Cadherin 13 became of particular interest because Cdh13 mRNA co-laminates with WF cell bodies in the lower SO. To determine whether Cdh13 is uniquely enriched in WF cells, we labeled Cdh13 mRNA in NTSR1-GN209-Cre;STP-YFP15-labeled SC slices. WF cells could be visualized using GFP-targeting antibodies after Cdh13 mRNA in situ hybridization using RNAScope. 91.78% of WF cells (Fig. 2.2 green) were found to express (Fig 2.2B, yellow) Cdh13 mRNA (Fig 2.2B red). There were also Cdh13 expressing cell bodies that were not GFP positive. However, these cell bodies resembled NTSR1-GN209-Cre WF cell bodies in their shape and size. It is likely that there is a population of WF cells that are not labeled by NTSR1-GN209-Cre that are Cdh13 expressing.

It is important to note that NTSR1 expression does not correlate with Cre expression in this mouse line since it is the BAC transgenic line. This is the case with the SC WF population as NTSR1 is not expressed in WF cells and other NTSR1-Cre mouse lines do not label WF cells (not shown). It is therefore notable that Cdh13 is a molecular marker for WF cells that represents the true expression of the population. To investigate the role of Cdh13 in WF cells as well as establish a molecularly relevant WF cell marker, we used a Cdh13-CreERT mouse line.

A   NTSR-GN209-CRE; STP1-YFP

B   NTSR-GN209-CRE; STP1-YFP

C
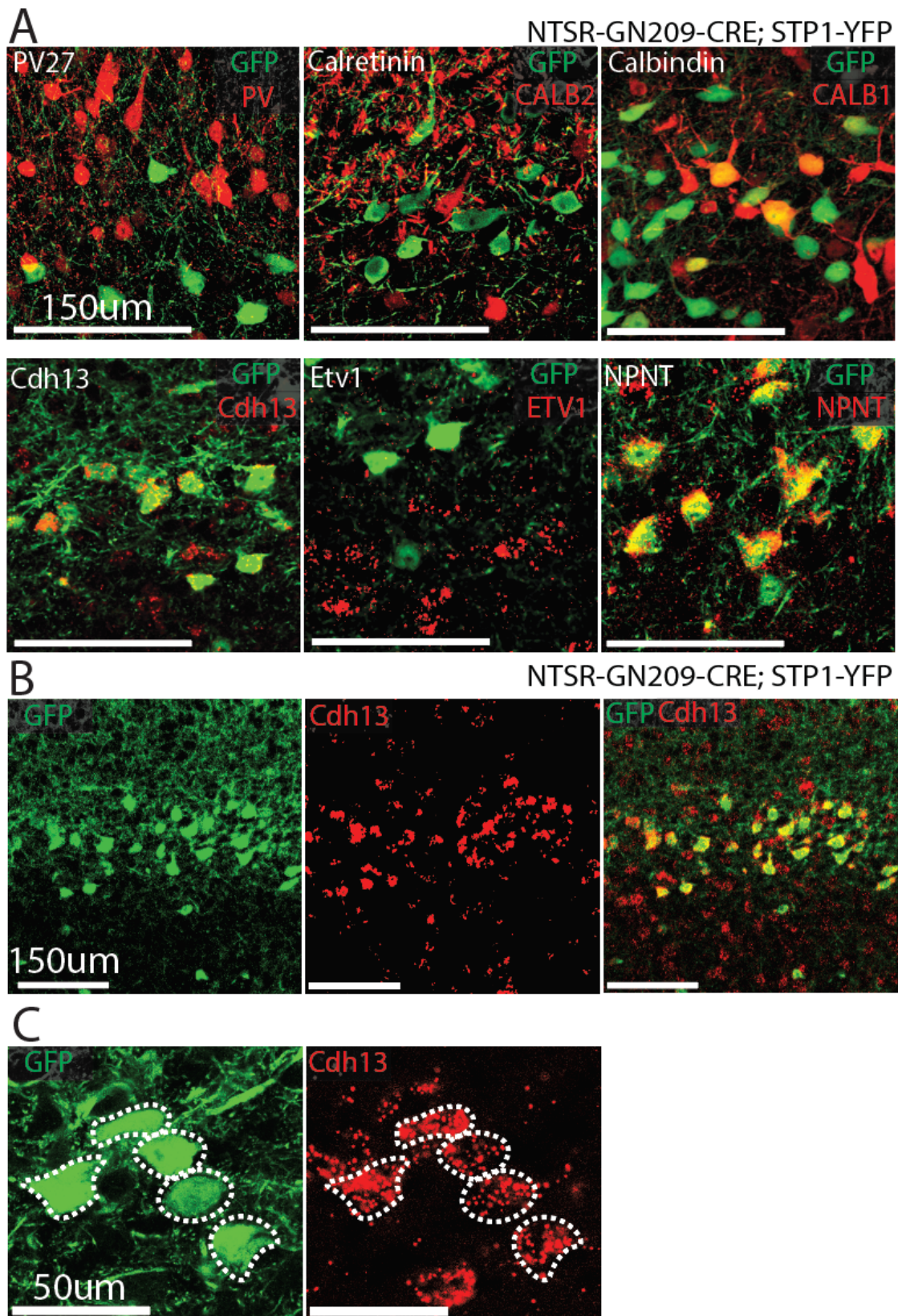
Figure 2.2. Molecular Characterization of Superior Collicular Wide Field Cells.

(A) Confocal images of NTSR1-GN209-Cre x Thy1-STP-YFP-15 labeled WF cells in eYFP. Molecular characterization of NTSR1-GN209-Cre labeled WF cells was determined through immunohistochemistry (top row) and in situ hybridization (bottom row) The percent of WF cells that express each molecular are: PV 0.11%; Calretinin 3.45%; Calbindin 24.76%; NPNT 87.00%; Cdh13 91.78%; ETV1 0.00%.

(B) Laminar restriction on Cdh13-expressing cell bodies (red) co-laminates with WF cell bodies (green).

(C) Cdh13 mRNA (red, right) is expressed in WF cell bodies (green, left)

Chapter 2.2: Cdh13 Expressing Cells are WF Cells.

To confirm that Cdh13 expressing cells in the sSC are WF cells, we used a Cdh13-CreERT;Stp-YFP15 mouse to visualize the anatomy of this population. Tamoxifen was administered IP beginning at p13 at 20ug/dose, every other day for 5 days, for a total of 3 doses. Earlier administration yielded a high mortality rate, while lower or later administration did not induce sufficient Cre expression. The Cdh13-Cre-ERT2 mouse line has the Cre-ERT2 domain inserted behind the Cdh13 promoter, disrupting the endogenous expression of Cdh13 while allowing for estrogen receptor bound CRE to be transcribed in cells that would otherwise express Cdh13 (Fig 2.5A). The heterozygous mouse would have one functional Cdh13 copy while the homozygous would have Cdh13 completely knocked out from conception. This results in the ability to consistently label the target population with or without endogenous Cdh13 expression in the heterozygous and homozygous mice respectively.

To confirm the Cdh13-expressing population labeled in this mouse line indeed labels NTSR1-GN209-Cre WF cells, we compared the cell body size and location, as well as dendritic spine densities between heterozygous Cdh13-CreERT;STP15 and NTSR1-GN209-Cre;STP15 mice. The labeled sSC population in the Cdh13-CreERT HET mice exclusively consisted of WF-like cell types with large cell bodies in the lower SO resembling that of NTSR1-GN209-Cre WF cells (Fig 2.3A). Both populations had complex dendrites that covered a large area reaching to the surface of the SC (Fig 2.3B). Both populations had no significant different in spine densities, with NTSR1-GN209-Cre WF cells having a spine density of 93.56±08.48 spines/mm; n=46 dendrites, while heterozygous WF cells had a spine density of 98.78±7.05 spines/mm; n=102 dendrites (p=0.6613) (Fig 2.3C). There was also no significant difference in spine distribution along the dendrite (Fig 2.3D, Fig 2.4). Through this, we concluded that the Cdh13-CreER mouse line labels WF cells in the superior colliculus.
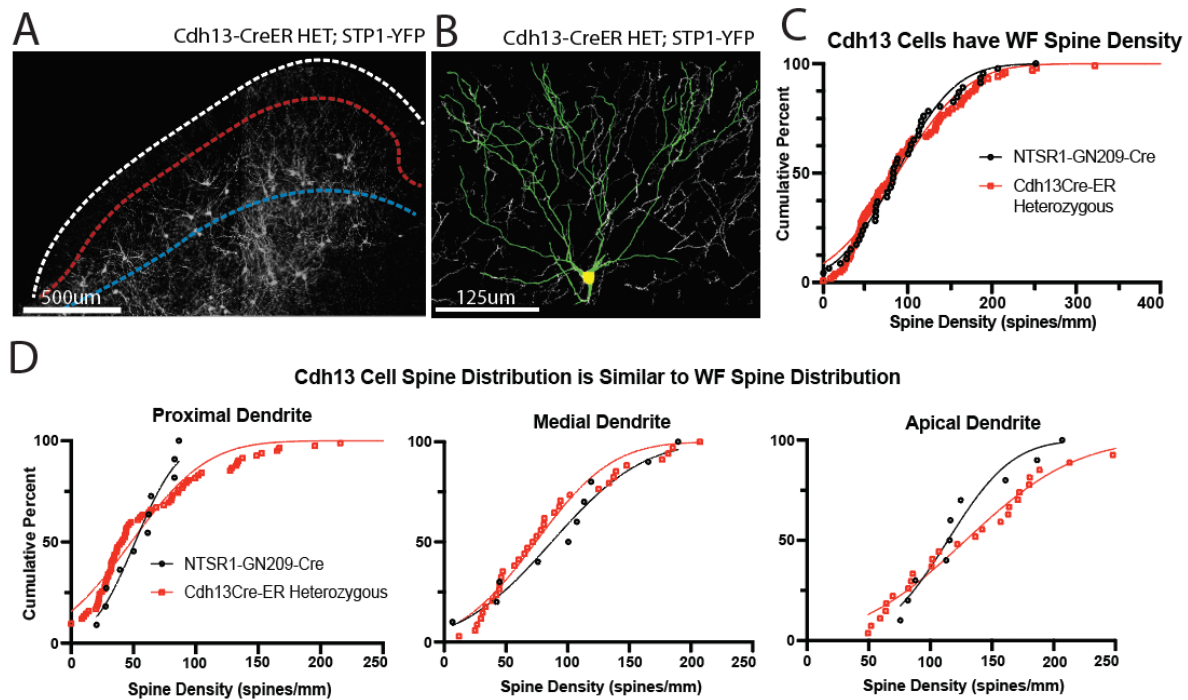
Figure 2.3. Cdh13-CreER labeled cells are WF cells.
(A) Confocal image of Cdh13-CreER mouse line labeled neurons. Labeled Cdh13 cell bodies are laminarly restricted to the lower SO like NTSR1-GN209 WF cells.
(B) Isolated Cdh13-CreER labeled cells have WF cell morphology.
(C) Cumulative percent graph comparing dendritic spine density between Cdh13-CreER Het labeled cells and NTSR1-GN209 labeled cells. There is no significant difference (n.s. p>0.05).
(D) Cumulative percent graphs comparing spine density distribution along the dendrite according to relative locations shown in Fig 7. Spine distribution between Cdh13-CreER cells and NTSR1-GN209-Cre is not significantly different at all locations. (p>0.05 for proximal, medial, and apical locations).
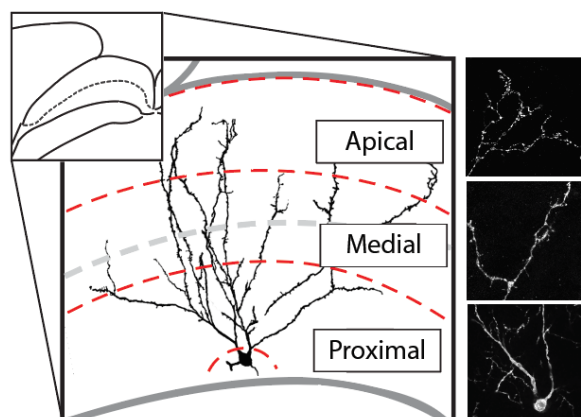
Figure 2.4. Scholl-like analysis is used to compare spine densities along the dendrite. (left) Diagram depicting proximal, medial, and apical dendrite boundaries. Boundaries are determined in a sholl-like analysis determined by the location of the cell body and surface of the SC surface, divided into 3 equal sections. (right)

Chapter 2.3: Cadherin-13 endogenous knockout results in a decrease in mature spines in WF cells

Cadherin 13 (Cdh13) is a GPI-coupled Type II cadherin involved in CNS axonal targeting and synaptic regulation (Ciatto et al., 2010; Kiser et al., 2019; Nguyen et al., 2020; Philippova et al., 2008). To determine the role of Cdh13 in SC WF cells, we analyzed changes when knocking out Cdh13 between our homozygous and heterozygous Cdh13-CreER mice. The homozygous mouse lacks Cdh13 mRNA expression (Fig. 2.5C green) while WF cells (labeled by NPNT mRNA in red (Tsai et al., 2022) show no changes in cell numbers or location (Fig 2.5C). The heterozygous mouse has one Cdh13 copy and robustly expresses Cdh13 mRNA (Fig 8B green), co-expressing (Fig 2.5B yellow) with WF cell bodies (Fig 2.5B red). We found that the heterozygous Cdh13-CreER mice, with one functional Cdh13 allele, were haplo-sufficient when compared to NTSR1-GN209-Cre WF cells in terms of total spine numbers and spine distribution along the dendrite (Fig 2.3D). NTSR1-GN209-Cre WF cells had a spine density of 93.56±8.48 spines/mm; n=46 dendrites while heterozygous WF cells had a spine density of 98.78±7.05 spines/um; n=102 dendrites (p=0.6613). Therefore, the heterozygous littermates are used as the control in this experiment.

In the homozygous mice, we observed a significant decrease in the number of spines per unit length of dendrite at an average of 39.30±5.07 spines/mm (n=66 dendrites), compared to heterozygous control spine densities at 98.78±7.04 spines/mm (n=102 dendrites) (p < 0.001) (Fig 2.6C). Classically, there are 4 major spine types: stubby, narrow, mushroom, and filopodia (Fig 2.6B). Mushroom spines are considered mature spines and are associated with housing a functional post synaptic density. They are defined by having a head larger than the neck of the spine. In this study, we observe a 5th spine type. This type, we call "Long Mushrooms", have a spine head that is wider than the neck, but the overall length is greater than its width, which is distinct from the classic mushroom morphology (Fig. 2.6B). Looking at density changes of each spine type, we observed significant

decreases in only mature spine density in the knockout 9.577±1.934 spines/um (n=102 dendrites) compared to control 47.49±3.444 spines/um (n=66 dendrites) (p<0.0001) (Fig 2.6D). There was no significant change in narrow, stubby, or filopodia. Given the importance of mature spines in efficient glutamatergic communication between neurons, the decrease of mature spines, specifically, strongly suggests the necessity of Cdh13 in communication to WF cells.
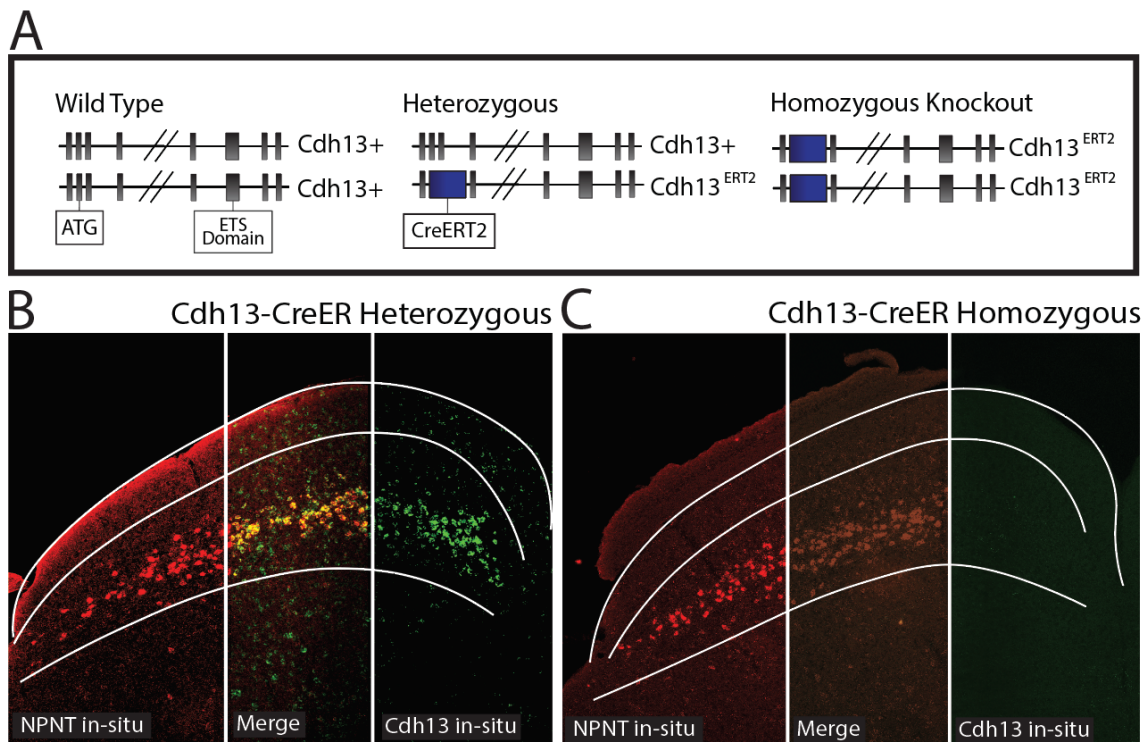
Figure 2.5. Knocking out Cadherin 13 reduces mature spines in WF cell dendrites.
(a) Genetic layout of Cdh13-CreER mice. The CreERT2 region is knocked into the transcription initiation region of the Cdh13-gene, knocking out functional Cdh13 transcription. The heterozygous mouse (middle) has one functional copy of the Cdh13 gene while a homozygous mouse (right) have a complete knockout of Cdh13 expression.
(b) Cdh13-CreER heterozygous mice continues to express Cdh13 mRNA in the appropriate lamina in WF cells. WF cells are labeled by NPNT mRNA (red, left) with coexpression with Cdh13 in yellow, middle.
(c) Confirmation of knockout in the homozygous but not heterozygous mice while maintaining WF cell laminar location and density. NPNT mRNA (red, left) lamination and density is maintained while Cdh13 mRNA (green, right) is abolished with no coexpression (yellow, middle).
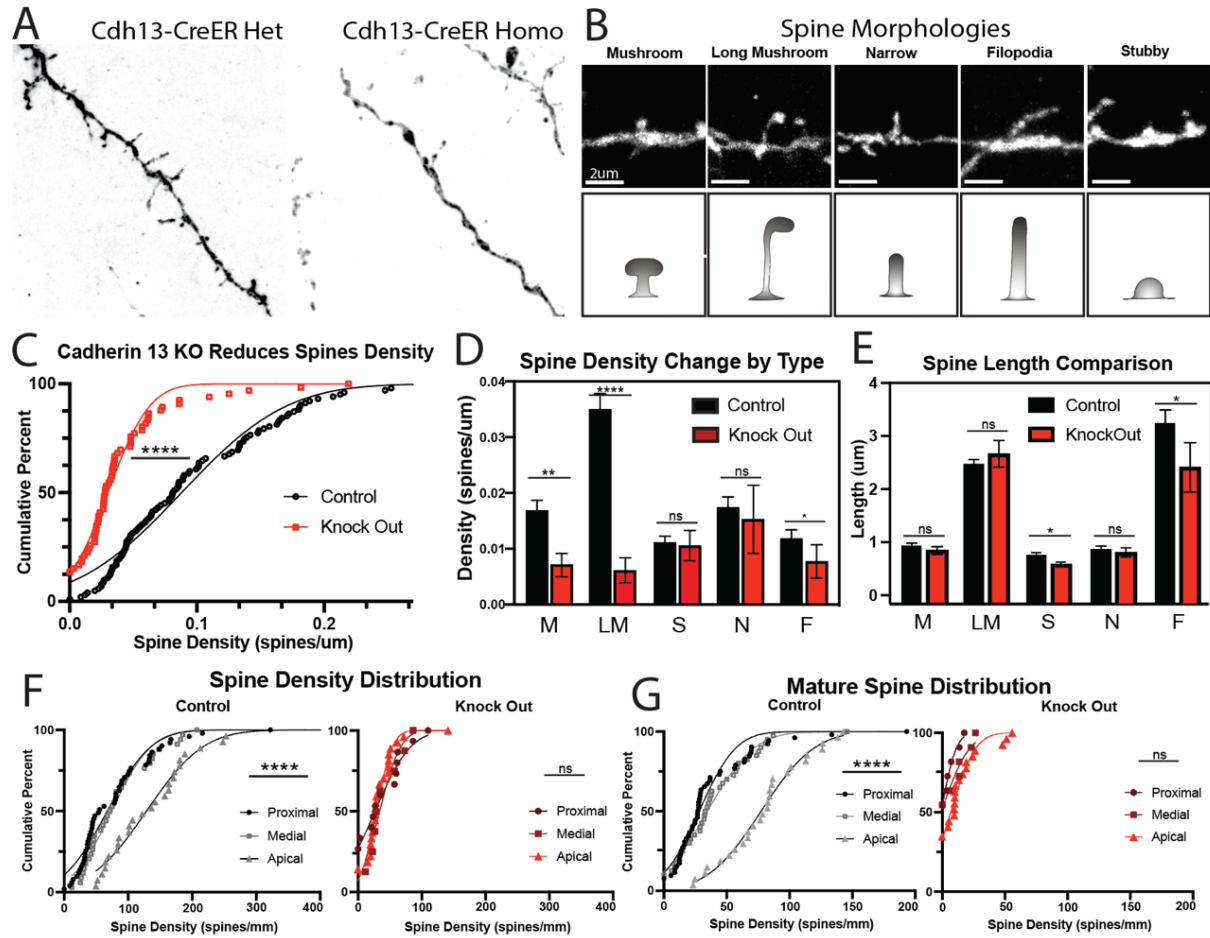
Figure 2.6: Knocking out Cadherin 13 reduces mature spines in WF cell dendrites.
(A) Dendritic spines are visible in both Cdh13-CreER heterozygous (left) and homozygous (right), with a decrease in the number of spines in the homozygous knockout condition.
(B) Five spine morphologies are observed in our Cdh13-CreER;StpYFP15 mice. (top) example images of spines from heterozygous mice. Each spine type was observed in homozygous samples as well (not shown) with no observable change in morphology.
(C) Cumulative percent distribution of dendritic spine density is significantly reduced when Cdh13 is endogenously knocked out (red) compared to the heterozygous control (black) ($p<.0001$).
(C) Comparisons of densities of each spine morphology show a significant decrease in mushroom ($p<0.01$) and long mushroom ($p<0.0001$) populations but not in stubby, narrow, or filopodia ($p>0.05$, $p>0.05$, $0.01<p<0.05$, respectively).
(E) Comparison of spine lengths show no change in lengths in mushroom, long mushroom, and narrow spines ($p>0.05$) with a small decrease in stubby and filopodia lengths ($p<0.05$).
(F) Comparison of cumulative percent distributions of overall spine densities at different locations along the dendrite from the cell body show a disproportionate decrease of spines in the apical regions in the knockout (right, reds) compared to the control (left, blacks).
(G) The disproportionate decrease in the apical regions is observed in mature spine distributions in knockout conditions (right, reds) compared to the control (left, blacks)
ns $p>0.05$, *$p<0.05$, **$p<0.01$, ***$p<0.001$, ****$p<0.0001$

Chapter 2.4: Apical dendritic spines are disproportionally affected by Cdh13 KO

sSC neurons and their inputs are highly laminarly organized. Is it therefore hypothesized that Cdh13-dependent mature spines could be concentrated at a specific lamina. To test this, a Scholl-like analysis was performed by dividing dendritic arbors into three zones according to their morphology and distance to the SC surface. The proximal region consists of thick primary dendrites in the lower 1/3 between the cell body and the surface of the SC. The apical region consists of thin, complex dendritic terminations in the upper 1/3 between the cell body and the SC surface. The medial region is the 1/3 between the proximal and apical regions consisting of "classical" dendritic arms of medium to thin thickness (Fig 2.4).

In control (both wild type NTSR1-GN209-Cre and Heterozygous Cdh13-CreERT WF cells), the apical region (142.20±17.8 spines/mm n=27 dendrites) has significantly more spines per length of dendrite than the proximal (78.78±8.72 spines/mm n=51 dendrites) and medial (84.45±8.96 spines/mm n=34 dendrites) regions in the control. In the Cdh13 knock out condition, the higher apical spine density was absent with all three regions having the same overall spine density (proximal: 36.42±9.0 spines/mm; medial: 42.40±9.38 spines/mm; apical: 33.8±5.46 spines/mm, fig. 2.6F). All three regions experienced a decrease in spine density, with the apical region observing the largest percent decrease. Mature spine distribution also observed a consistent trend., with a larger percent decrease in apical regions in the absence of Cdh13 (12.65±3.106 spines/mm) when compared to the control (79.91±6.388) (Fig. 2.6G). Taken together, these results indicate that Cdh13-dependent mature spines are present throughout the entirety of WF dendrites, but there is a higher density of them in the apical dendrites in the superficial SGS. It is therefore possible that communication between populations innervating the upper SGS and WF cells are Cdh13-dependent.

One consideration in interpreting these observations is the possibility that there are changes in the dendritic arborization when Cdh13 is knocked out. There may be changes in dendritic laminar targeting or dendritic complexity. Although if these changes occurred, the fact that we see changes to spine density does not change. What does change is the interpretation of this phenotype. For example, if Cdh13 removal results in dendrites no longer being in a region where they normally make axonal contacts, it is possible that the loss of spines is because of the mislocalization itself, rather than at the spine itself. On the other hand, if dendritic morphology is unaffected, it is more likely that Cdh13 is involved at the spine level.

Due to the size and breadth of WF cell dendrites, many dendrites are severed before reaching their natural termination. Therefore, analyzing cell reconstructions for changes in dendritic arborization would not be an accurate representation. So any changes when knocking out Cdh13 would be misleading. To circumvent this issue, we analyzed the ratio of dendritic densities between proximal, medial, and apical regions and compared them between control and knockout conditions. Comparisons of the ratio between the regions is necessary because tamoxifen induction of Cre expression results in variable densities of cell labeling between mice. Assessing changes in this way allows for appropriate analysis of changes in dendritic laminar targeting and termination. We found that there were no changes in dendritic laminar targeting between Cdh13 knockouts and their heterozygous littermates.

This analysis method does not tell us whether there is a change in dendritic complexity due to Cdh13 knockout. Although there were no observable changes in the number of primary dendrites, it was difficult to quantify possible changes in dendritic complexity. Qualitatively, there appeared to be no notable changes in dendritic complexity (Fig 2.1). Regardless, if there were changes in dendritic complexity, the significant reduction in mature spine density and its interpretation would not greatly change since no laminar defect was detected. The WF dendrites would still innervate all endogenous

SC layers and therefore would have the opportunity to contact their appropriate partners for proper synapse formation or spine maturation. Therefore, the changes in the spine due to Cdh13 knockout would be a result of abolishing Cdh13's action in spine morphology.

Chapter 2.5: Cadherin 13 is necessary in adult WF spine maintenance

Cadherin 13 expression robustly persists in the sSC WF through adulthood (Fig. 1.1D). This raises the question of whether continued Cdh13 expression is necessary for mature WF spine maintenance after development. To address this, we developed a virally mediated shRNA targeting Cdh13 mRNA (Fig 2.7A). This protein was complexed with a cleavable Cre-dependent mCherry (pAAV-hU6-shCdh13-DIO-mOrange2). The knockdown sequence was adapted from Killen et al. (2017). We knocked down Cdh13 in SC WF cells by injecting this virus into p60 NTSR1-GN209-Cre superior colliculi in mice (Fig 2.7A). mCherry was observed in only WF cells in the SC. Cdh13 mRNA knockdown was confirmed via in situ hybridization (Fig 2.7B). NPNT(+);RFP(-) cells were Cdh13(+), while all RFP(+) cells were NPNT(+) but Cdh13 negative (Fig 2.7C). Like the endogenous knockout condition, no changes in cellular lamination or cell numbers were changed from the control.

In the Cdh13-knockdown population, overall spine density (28.79±03.54 spines/mm, n=56 dendrites) was significantly decreased when compared to NTSR1-GN209-Cre WF cell control (98.78±7.05 spines/mm, n=102 dendrites) (n<0.0001). The knockdown density was comparable to that of the endogenous knockout (39.30±5.07 spines/um; n=66 dendrites). Unlike the results from endogenous knockout conditions, adult Cdh13 knockdown significantly reduced the populations of all spine types (Fig 2.7G). However, mature spines were consistent in having a larger percent decrease than other spine types.

The same experiment was conducted on Cdh13-CreER;STP15 mice in order to specify knockdown to only Cdh13-expressing WF cells. Mice were injected in one SC hemisphere at p1 using a glass pipette. Tamoxifen was then administered beginning at p15. Brain tissue was then collected 4 weeks later. The resulting decrease in spine density was similar to the p60 knockdown, showing a general decrease in all spine types but a greater percent decrease of mature spines, with the greatest area of effect being in the distal apical dendrites.

These results show that adult Cdh13 disruption reduces mature spine density, similar to the endogenous Cdh13 knockout. Given that Cdh13 is necessary after development in this system, it can be concluded that Cdh13 is necessary for the maintenance of these mature spines. In addition, since the shRNA virus was not axonally taken-up by RGCs (Fig 2.7D) or V1 cortical cells that also innervate the sSC (May, 2006), the knockdown was exclusive to Cdh13-expressing cells in the SC. Therefore, Cdh13 knockdown in the adult WF cells is sufficient to decrease mature spine numbers. Taken together, this demonstrates that Cdh13 is necessary in the adult SC to maintain mature dendritic spine anatomy.

A

Mouse: NTSR-GN209-Cre
Age: p60

B AAV2-shCdh13-2A-DIO-mCherry
NTSR1-GN209-Cre

500um

RFP

C AAV2-shCdh13-2A-DIO-mCherry Injected SC WF Cells

RFP

NPNT

Cdh13

50um

D NTSR1-GN209-Cre Retina

E Adult Cdh13 KnockDown

****

Control
Adult Knockdown

Spine Density (spines/mm)

F Density by Location

Control

***

Proximal
Medial
Apical

Spine Density (spines/mm)

KnockDown

ns

Proximal
Medial
Apical

Spine Density (spines/mm)

G Spine Density by Type

Mushroom   Long Mushroom   Stubby   Narrow   Filopodia

Control   Adult Knockdown   Endogenous Knockout

Figure 2.7: Continued Cdh13 expression is necessary for mature spine maintenance.

(a) Genetic scheme of viral Cdh13 shRNA knockdown with Cre-dependent mCherry. This is injected into the SC of a p60 NTSR1-GN209-Cre mouse.

(b) Confocal image confirming infection of WF cells specifically at point of injection into the adult SC. AAV2-shCdh13-77-2A-DIO- mCherry infects WF cells and expressed mCherry.

(c) Confocal image of infected WF cell to confirm Cdh13 knockdown only in infected cells. RNAscope in situ hybridization shows mCherry expressing WF cells (NPNT+ cells) are absent of Cdh13 mRNA.

(d) Confocal image of the retina of SC injected mice to show lack of axonal uptake of shCdh13. Lack of mCherry in Cre+ RGC Cells in the retina indicate lack of retrograde transport to the retina (0% RFP+ Cells, n = 6 eyes, 3 mice).

(e) Cumulative percent of spine density comparison show decreases in spine density after adult Cdh13 shRNA knockdown. Control is NTSR1-GN209-Cre labeled WF cells.

(f) Comparison of spine density distribution along the dendrite between control (left) and knockdown (right) conditions.

(g) Comparison of spine density by type. Control is NTSR1-GN209-Cre, knockdown is virally mediated sh knockdown, and endogenous knockout is homozygous Cdh13-CreER from figure 9.

ns $p > 0.05$, *$p < 0.05$, **$p < 0.01$, ***$p < 0.001$, ****$p < 0.0001$

Chapter 2.6: Cdh13 Expressing RGC population has dendritic and axonal laminar specificity.

In the CNS, Cadherin 13 is an exclusively homophilic actor (Ciatto et al., 2010; Ranscht & Bronner-Fraser, 1991; Spranger et al., 2006; Vestal & Ranscht, 1992) in maintaining transsynaptic stability (Killen et al., 2017; Kiser et al., 2019; Rivero et al., 2015; Tantra et al., 2018). We therefore hypothesized that spine density in WF cells is dependent on presynaptic Cdh13 expression. To determine whether presynaptic Cdh13 disruption reduces WF mature spine numbers, it was first necessary to identify a candidate presynaptic population. Retinal ganglion cells prominently innervate the superficial SC. 90% of retinal projections target the sSC in the mouse and 10% in primates (Perry & Cowey, 1984). We used our Cdh13-CreER-StpYFP mouse line to visualize Cdh13-expressing retinal cells via tamoxifen injection. Immunohistochemical stains determined that 100% of GFP labeled RGCs were RBPSM+. Of these 47.6% were sabt1+, 0% were CART+, and 2.86% were OPN+, non-exclusionary. Accordingly, Cdh13 mRNA was stained to show expression in 6.67% of KCNG1-Cre RGC and 96.78% in W3-GFP RGC.

Analysis of Cdh13-RGC anatomy observed small cell bodies with dendritic stratifications in IPL S3 in the majority of cells with some having additional stratifications varying from S1-S5. These dendritic anatomies resembled W3b RGC (Kim et al., 2010), F-midi RGCs, and F-mini RGCs. Cdh13 expression in F-RGCs is consistent with previous reports (Rousso et al., 2016)(Fig 2.8A) but Cdh13-expression in W3-RGC has not been previously reported. Cdh13-RGC axons laminate in the upper SGS and mid sSC respectively (Fig 2.8B). No axons were observed to terminate in the SO. This axonal lamination further supported the dendritic data indicating that this population includes W3b-RGC and F-RGCs.

Based on the molecular and anatomical data we gathered, the Cdh13-expressing population predominantly consists of W3b RGCs and F-RGCs while excluding alpha RGCs. It is unclear to what degree this population encapsulates the entirety of W3 and F populations, but it is certain that some

portion is Cdh13 expressing. For this study, we will consider all Cdh13-expressing RGCs labeled in our Cdh13-CreER;STP15 mouse line as a single population and will be analyzed as such in subsequent experiments.

A Cdh13-CreERTHET;Thy1STP-YFP-15

W3

F-ON mini

50um

50um

50um

50um

B Retinal AAV2-Dio-GFP Injection

GFP

C

200um

GFP + RFP

Retinal AAV2-shCdh13-2A-DIO-mCherry

30um

50um

E Change in Spine Density After Retinal Cdh13 KnockDown

Mature Spine Density

Non-Mature Spines

Cumulative Percent

Spine Density (spines/mm)

Control Zone
Knockdown Zone

**

ns

Control Zone
Knockdown Zone
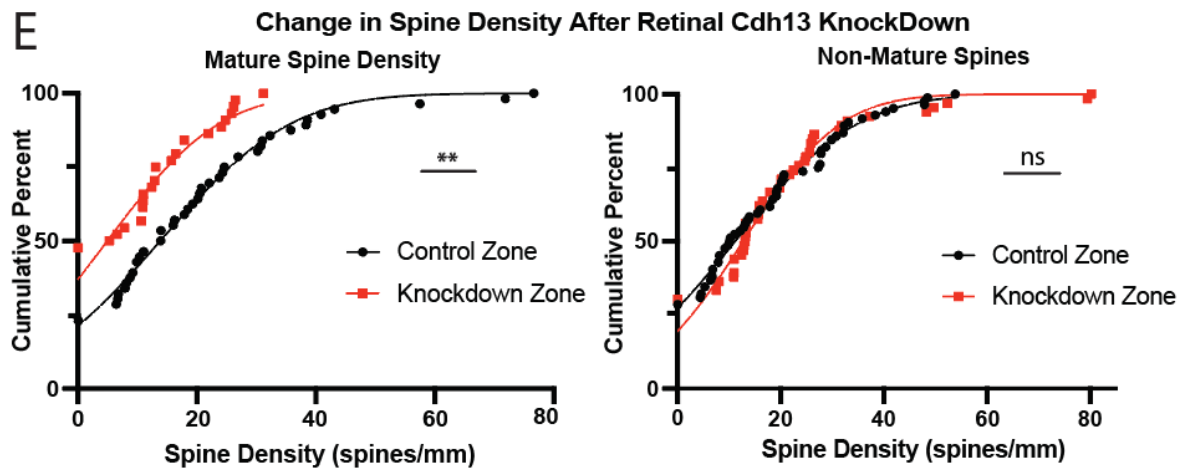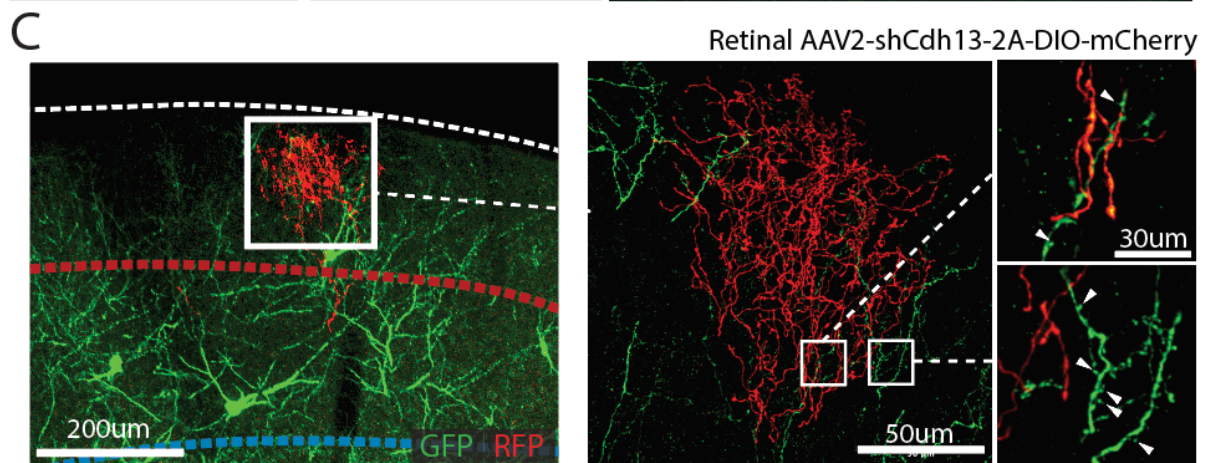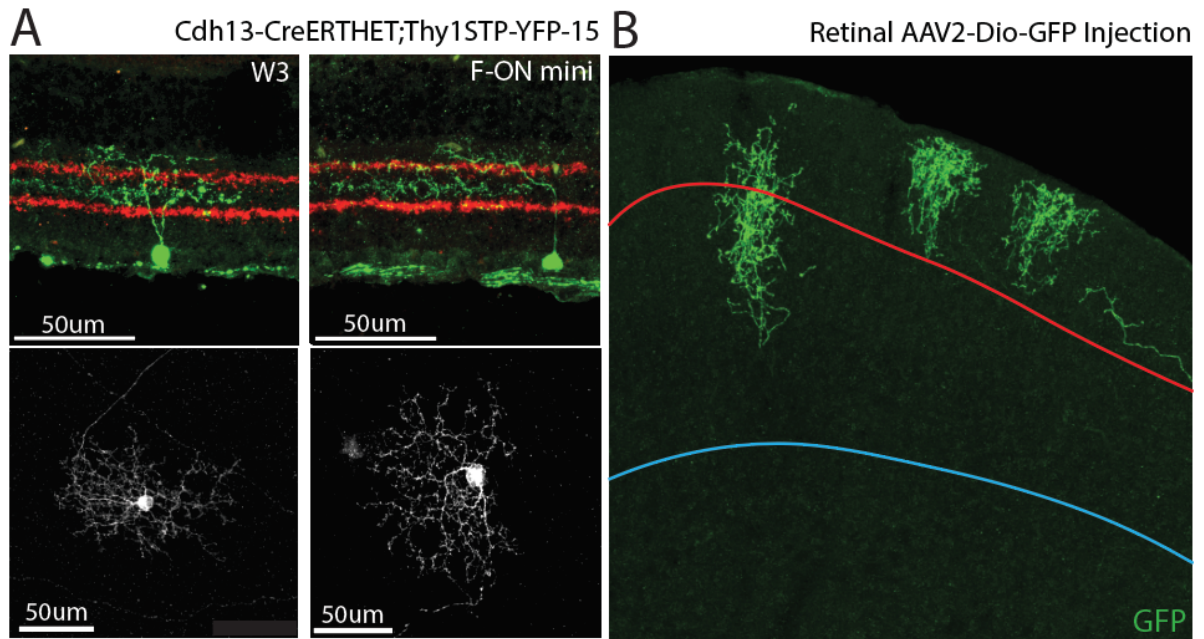
Figure 2.8: Retina specific Cdh13-KnockDown locally reduces mature spines at Cdh13-RGC axonal terminal zones.

(a) Confocal images of Cdh13 expressing RGCs labeled by Cdh13-CreER Heterozygous; StpYFP15 in the retina. Cdh13-RGCs predominantly have anatomy resembling W3-RGCs and F-on Mini RGCs. Homozygous samples observe similar morphologies (not shown).

(b) Confocal image of Cdh13-RGC axons that are labeled by AAV2-DIO-GFP in Cdh13-CreER Heterozygous mice. This method allows for Cdh13-RGC axonal isolated labeling in the SC without Cdh13-WF dendrites. Majority of Cdh13-RGC axons terminate in the upper SGS with some along the SGS/SO boundary. This lamination coincides with W3-RGC and F-RGC axons.

(c) Retinal injection of AAV2-DIO-shCdh13-mCherry labels RGC terminals in the SC. (left) 10x image of RFP labeled axon in the SGS. (mid) 40x of RGC axons (right) comparison of RFP axon innervated (top) and non-innervated Cdh13-WF dendrites (green). Mature spine numbers labeled by white arrows.

(d) Cumulative percent plots of spine densities of (left) mature spines (mushroom/long mushroom) and (right) non-mature spines (narrow, stubby/filopodia).

Chapter 2.7: Retinal Ganglion Cell Cdh13 knockdown locally reduces spine density.

To determine whether presynaptic Cdh13 in RGCs is necessary for mature spine densities in WF cells, we knocked down Cdh13 by injecting the same pAAV-hU6-shCdh13-DIO-mOrange2 intravitreally in our Cdh13-CreER;STP15 mice. This allowed for Cdh13-knockdown in Cdh13 expressing RGCs after tamoxifen administration. Mice were injected at p0-2, tamoxifen induced beginning at p15, and then were humanely sacrificed and retinal tissue collected 4 weeks after tamoxifen. Identification of infected Cdh13-RGCs and their axons was achieved through RFP immune-labeling and WF cell dendritic visualization was achieved in the same sample with GFP immune-labeling. GFP-only RGC axons were difficult to visualize since their GFP expression is significantly dimmer than that of WF cell dendrites (not shown). RFP+ axons were GFP+, however this was only observable after the RFP was photobleached under 2photon lasers under a confocal microscope. Polygonal zones were drawn around RFP+ axonal areas in the SC. These zones were defined as areas with presynaptic Cdh13 knockdown (Fig. 2.8C). The GFP+ dendrites in these zones would be analyzed in opposition to GFP+ dendrites outside of these zones. It is also notable that RFP+ axons did not change axonal lamination despite the knockdown of Cdh13 (Fig 2.8C). Although this may be a factor of the age of knockdown onset, endogenous knockout RGC axons do not shift lamination either (Fig. 3.4A). Therefore, it is unlikely that Cdh13 is involved in axonal targeting in the SC.

In the presynaptic knockdown zones, there is not a significant populational decrease in total WF spine density between the knockdown zones (56.64±9.807 spines/mm n=22) and the surrounding control areas (79.42±10.93 spines/um n=28). However, when specifically comparing individual spine types, mature spines (mushroom and long mushroom) populations were decreased in RFP+ knockdown zones (8.50±1.46 spines/mm n=22) compared to control zones (17.66±2.33 spines/um

n=28) (Fig 2.8E). This trend was exclusive to mature spine types with no change observed in stubby, narrow, or filopodia spines.

These results indicate that the removal of retinal ganglion cell Cdh13 reduces the dendritic spine density of WF cells exclusively in their axonal termination zones. This strongly suggests a mode of homophilic interaction dictating Cdh13 action in spine morphology. This data also elaborates on the role of Cdh13 in maintaining mature spines in WF dendrites since WF and retinal knockdown were conducted in adult mice. It can therefore be concluded from the data that Cdh13 is necessary for mature spine interaction between specific RGC populations and SC WF cells in a homophilic manner.

DISCUSSION

Understanding how cadherins direct cell type-specific connectivity requires an understanding of cadherin expression patterns of innervating and receiving populations. In previous work cadherin 8 and 9 (Duan et al., 2014) and cadherin 6, 9 and 10 (Duan et al., 2018) retinal expression patterns were determined before identifying how these cadherins direct specific connectivity. In the current study we surveyed SC cadherin expression in established anatomical cell types to determine a unique enrichment of Cdh13 in WF cells (Fig 2.2, 2.3, 2.4). We found that endogenous Cdh13 KO reduces mature spine density, with a greater proportional loss in apical regions (Fig 2.6). A similar loss was observed in adult Cdh13 local shRNA knock-downs in the SC (Fig 2.7). When cdh13 was knocked down in Cdh13-expressing RGCs, mature spine densities were decreased in affected axonal termination zones but not in surrounding areas (Fig 2.8). Taken together, Cdh13's restricted expression in RGC and SC populations allows for cell type-specific interactions. This interaction directs critical synaptic anatomy. Cdh13 then maintains these interactions well into adulthood.

Anatomical Changes Suggest Functional Changes

Dendritic spines are the primary site of glutamatergic input in the CNS and their reduction has been shown to negatively affect synaptic function (Boros et al., 2019; Boros et al., 2017; Walker et al., 2021). For retinal-tectal connectivity, glutamatergic input is extremely important as retinal ganglion cells are glutamatergic. In excitatory neurons, most glutamatergic synapses are made on the heads of dendritic spines, each of which houses the postsynaptic terminal of a single glutamatergic synapse (Alvarez et al., 2007). Therefore, the existence and maintenance of the primary glutamatergic input structures in the superior colliculus are critical for the communication of visual information from the retina to the SC.

Although a loss of spines does not necessarily indicate a removal of synaptic connectivity, it has been shown that changes in spine morphology or number greatly affects the functionality of synaptic communication. Chemically-induced actin depolymerization reduces spine size and numbers while also reducing synaptic transmission and blocking LTP and LTD (Okamoto et al., 2004). Although functional changes in relation to morphological changes seem to be restricted to the individual spine itself, as a collective population within the cell, spine head size and synaptic enhancement show a positive correlation (Hayashi & Majewska, 2005; Matsuzaki et al., 2004). Nevertheless, there is evidence showing that changes in spine morphology and number affects behavior (Gipson & Olive, 2017). Accordingly, the loss of spine numbers is a common feature of early neurodegenerative diseases such as Alzheimer's (Boros et al., 2019; Boros et al., 2017; Walker et al., 2021). Therefore, the observed loss of dendritic spines indicates a significant likelihood of Cdh13-dependent change in communication between Cdh13-expressing RGCs and WF cells.

Development vs Maintenance

Knocking down Cdh13 in mice that are well past the development stage resulted in a reduction of spine number comparable to the endogenous Cdh13 knockout. Given the time frame of the knockdown, we conclude that Cdh13 is necessary for the maintenance of mature spines in WF cells. Although there are some instances of adult spinogenesis, it is rare. In addition, mature spines have been found to be relatively immotile when compared to their immature relatives (Alvarez et al., 2007). Filopodia are the most dynamic as they can appear and disappear in as little as 10 minutes (Ziv and (Ziv & Smith, 1996). Stubby spines could be mushrooms that undergo neck reduction, but overall, this need to be reevaluated (Tonnesen et al., 2014). Stubby and thin spines are less dynamic than filopodia and can persist over several days (Holtmaat et al., 2005). On the other hand, mushroom spines can be stable over several months (Grutzendler et al., 2002). Therefore, a reduction of mature

spines when Cdh13 is knocked down in p60 adult mice is notable. Taken together, this indicates that a loss of Cdh13 causes a deficiency in the maintenance of existing spines, rather than a decrease in adult spinogensis.

However, there is the possibility that Cdh13 has a role in spinogenesis during development in addition to maintenance in adulthood. There are multiple theories of how spines form during development. The true mechanism may vary depending on the CNS region and cell type. The Sotelo model (Sotelo, 1990) states that immature spines are developed before contact with an innervating axon causes maturation. The Miller/Peters model (Miller & Peters, 1981) states that mature spines develop when an innervating axon contacts the spineless dendrite, and immature spines are intermediate steps in the development. The Filopodial model (Vaughn, 1989) hypothesizes that filopodia reach out to contact the axon to "pull it down" to develop a synapse on a mature spine. Each model has supporting evidence and their implementation may vary across the CNS (Fiala et al., 1998; Hirano & Dembitzer, 1973; Landis & Reese, 1977; Rakic & Sidman, 1973; Sotelo, 1975; Vaughn et al., 1974). Depending on the model employed, the phenotype resulting from a disruption in any step in the development will be different. If Cdh13 were involved in either immature spine development or their maturation in the Sotelo model, the knockout would result in less spines of every category or more immature spines with less mature spines respectively. In the Miller/Peters model, if Cdh13 were involved in axonal contact with the dendrite or any part of spine development into a mature spine, Cdh13 knockout would cause an overall decrease of all spine types in both scenarios. And in the filopodial model, if Cdh13 were involved in filopodial outgrowth or spine maturation after filopodial contact, we should see a decrease in mature and filopodial spines or an increase in filopodia with a decrease in mature spines respectively. However, our endogenous knockout results only show a significant decrease in mature mushroom and long mushroom spines, without any large changes to narrow, stubby or filopodia spines. This suggests that Cdh13 is not involved in any of these

developmental steps in any of these predominant spinogensis models. Therefore, it is reasonable to hypothesize that Cdh13 is either involved in a model of spinogensis that has not yet been described, or it is not involved in the development of spines in this manner.

However, one hypothesis is that Cdh13 is necessary for maintaining spines against the pruning of supernumerary synapses during development. This would mean that mature spines formed initially during development would be pruned in the absence of Cdh13's anchoring mechanism. An illustration of the proposed mechanism is presented in Figure 2.9. Cdh13 resides in lipid rafts, a structure that is known to concentrate synapse-related proteins. Cdh13 would then bind homophilically with the transsynaptic cell to anchor the structures in place. In the event of pre- or post- synaptic loss of Cdh13, this study showed that mature spine numbers were decreased, specifically in the area of effect. This could be caused by the lack of synaptic protein anchoring, causing spine pruning. However, it is possible that this loss of spine morphology does not result in a loss of synaptic connection. A robust time course of the dendritic spine development with functional or transsynaptic studies would be needed to properly address this hypothesis.

Nevertheless, the data supports the conclusion that Cdh13 is indeed necessary for the continued existence of mature spines in WF cells in the SC in the adult. And given the relatively low level of spinogensis in adulthood, it is reasonable to further conclude that Cdh13 is involved in the maintenance in these spines rather than spinogenisis past development.
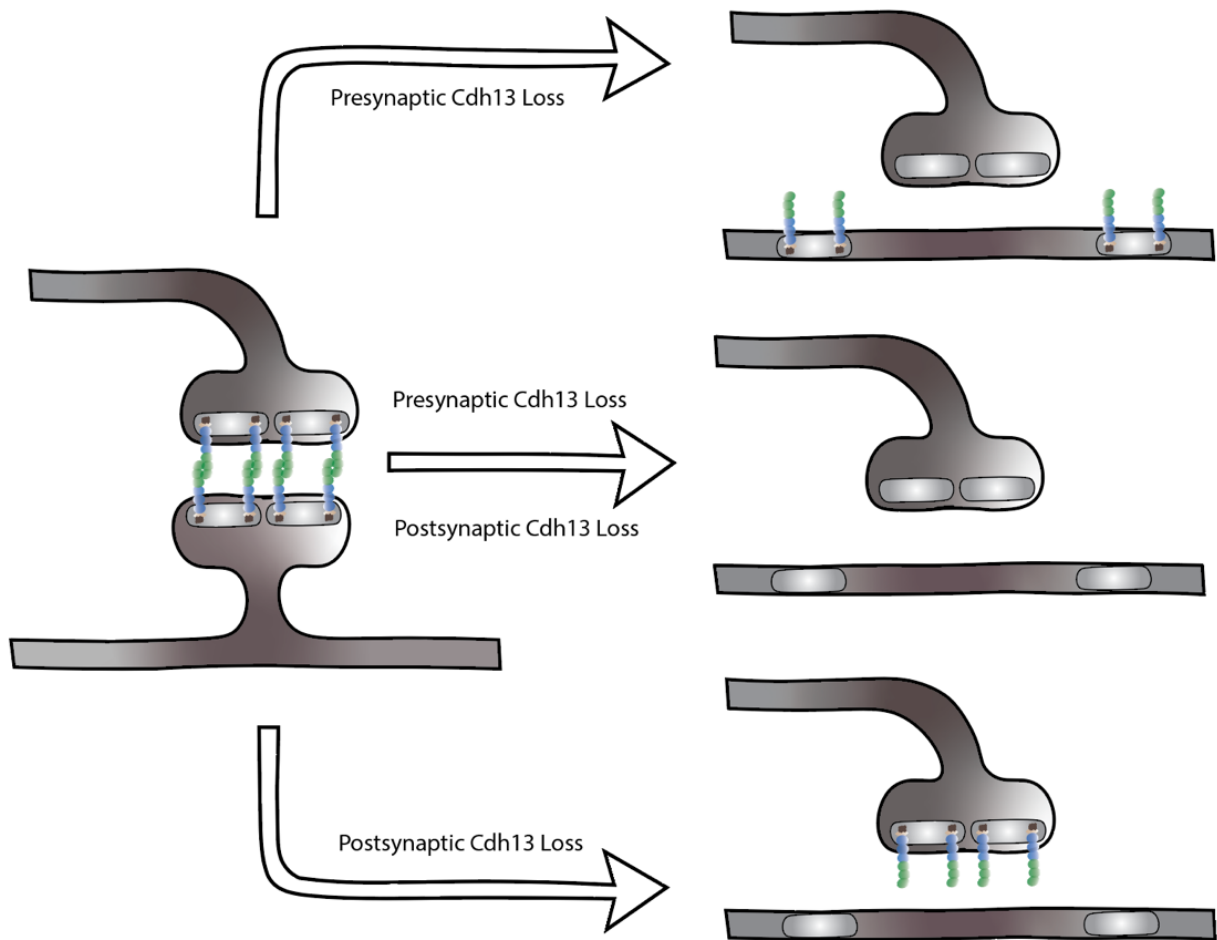
Figure 2.9. Proposed mechanism for Cdh13 function at synapse.
Cadherin 13 is exclusively homophilically binding in the CNS. Given it's GPI moiety, it is hypothesized to be associated with lipid-raft dependent spine and synapse maintenance through homophilic, transsynaptic anchoring. This would require both pre-and post-synaptic Cdh13 expression.

Potential Compensatory Circuits

An interesting observation is the decrease of all spine types in the adult knockdown while the immature spines were unaffected in the endogenous knockdown. This is likely due to a reduced capacity for the neurons to compensate for the loss in adulthood while endogenous knockout conditions would be able to take advantage of increased developmental flexibility. Compensation for the loss of a cadherin function by other cadherins to maintain structural and functionality has been shown in previous retinal studies (Duan et al., 2018). When cadherin 6 and 10 were knocked out in On-Off Direction selective RGCs, no laminar or functional change was observed. However, there was an increase in Cdh9 expression in these cells. It was found that in the absence of Cdh6 and Cdh10 in this population, Cdh9 expression is upregulated and was able to compensate to maintain appropriate circuit wiring. Only upon deletion of Cdh6, Cdh9, and Cdh10, was there a phenotypic change observed.

It is likely that in the endogenous knockout condition, narrow, stubby, and filopodia spines are maintained through compensatory mechanisms. However, in the adult knock down, the less plastic neuron is unable to compensate for the loss of Cdh13, resulting in the loss of all spine types. It is unclear whether this loss occurs from loss of Cdh13 in these spines themselves, or whether they are a secondary byproduct of mushroom spine loss and the functional changes that brings. Confirmation of this hypothesis would require further study and identification of potential compensatory actors.

Retinal Identity/Circuit Function

We observed that almost all Cdh13 expressing RGCs have S3 IPL terminating dendrites and SGS terminating axons. Their IPL laminar restriction in the retina suggests that this population receives similar bipolar cell input, likely from type 5 bipolar cells (Ghosh et al., 2004; Tsukamoto & Omi, 2017). Their consistent axonal termination also suggests that Cdh13-RGCs target a similar population in the SC, given the laminar organization of SC populations. Moreover, RGCs with SGS terminating axons typically have direction-selective and object-detection preferences (Dhande & Huberman, 2014; Huberman et al., 2009; Kay et al., 2011; Kim et al., 2010; Kim et al., 2008; Rivlin-Etzion et al., 2011). Therefore, it is likely that the Cdh13-RGCs would have similar visual detection preferences given their specified input and output partners as defined by their laminar specification.

These theories were further corroborated by our anatomical analyses of Cdh13-RGC dendritic morphologies. We found that Cdh13 RGC population is largely represented by W3b-like and F-like RGCs. W3-RGCs respond to small moving stimuli and are theorized to be overhead threat detectors in mice (Zhang et al., 2012) and F-RGC minis are highly direction-selective (Rousso et al., 2016). This contrasts with alpha RGCs, a population not represented in Cdh13-RGCs, that respond to center surround stimuli and are not direction-selective (Huberman et al., 2008). Given the restricted population expressing Cdh13, it is therefore likely that Cdh13-RGCs convey a limited and specific type of information, likely, direction-selective object-detection possibly relating to predator-detection.

It is interesting to note that WF cells have been shown to be tuned to slow-moving, small stimuli (Gale & Murphy, 2014). Given their dendritic arbor size, they are able to detect small slow-moving objects over a large receptive field (Gale & Murphy, 2014). Hypothetically, it is representative of a predator flying overhead. Indeed, large bodied, LP targeting SC cells have been found to direct visually based fear responses to overhead stimuli (Shang et al., 2018). Given that the only sSC cell found to target LP are WF cells (Dhande & Huberman, 2014; Gale & Murphy, 2014), and given the

size and location of the cell bodies observed in the population in the study, it is likely that the experimental population were WF cells. NTSR1-GN209-Cre WF cells have also been shown to be involved in prey detection, specifically in visual detection and orientation when the prey was at a distance (Hoy et al., 2019). In other words, the detection of a small object over a large visual field.

Although de novo direction-selectivity in the CNS has been observed (Lien & Scanziani, 2018) it is expected that direction-selective visual information from a population would be passed to its downstream partners. Therefore, it could be hypothesized that the downstream partners of Cdh13-RGCs consisting of W3-RGCs and F-RGCs would also be sensitive to small, moving, objecting in a direction selective manner. Conversely, it is highly possible that WF cells derive their preference for small, direction-selective moving objects from presynaptic information. Our data suggests that the presynaptic Cdh13 of Cdh13-RGCs is necessary for the maintenance of mature spines on Cdh13-expressing WF cells. Given the importance of mature dendritic spines on glutamatergic synaptic transmission, it is hypothesized that the removal of Cdh13 from this system significantly affects the synaptic communication between Cdh13-RGCs and Cdh13-WF. Cdh13's role in the communication between these two functionally and behaviorally linked populations greatly suggests a critical behaviorally relevant role of Cdh13 in visual processing. Behavioral experiments detailing the effects of Cdh13 knockout in the retinal-tectal circuit are necessary to properly shed light on the functional necessitates of Cdh13.

Cadherin-13 vs NPNT in the SC

In Tsai et al 2022 we detail the role of NPNT in retinal-tectal wiring. There, NPNT-Itg8 signaling between the NPNT of SC WF cells and the Itg8 of aRGCs are shown to be mutually necessary for aRGC axonal targeting and restriction to the appropriate SO lamina. Interfering with the expression of either protein causes ectopic aRGC axonal targeting as well as a disruption of aRGC-WF communication. It was concluded that NPNT-Itg8 signaling was necessary for the axonal laminar restriction, but it was inconclusive whether it had a direct role in maintaining synaptic connectivity. It was theorized that the resulting disruption of the proximity of other molecules, such as cadherins, could be causing the loss of connectivity.

Here, we show that RGC-WF Cdh13 is necessary for the maintenance of spines without effecting the laminar restriction of Cdh13-RGC axons (Fig 2.3, 2.7, 3.3A). Therefore, conversely to NPNT-itg8 signaling, there must be a separate mechanism in place for axonal targeting. In addition, based on our data we theorize that Cdh13 is only involved in spine maintenance, rather than spinogensis, meaning non-Cdh13 mechanisms must be in place for the initial development. Although Cdh13 and NPNT systems are working in the same population of WF cells, they have different functions in directing connectivity between different RGC subtypes. Both molecules are examples of molecules that are necessary for the final transsynaptic connectivity, but individually have a very specific role. Nevertheless, both are necessary for the appropriate development and maintenance of a functioning behavioral and functional circuit.

Generalization/Relationship to Disease

The role of Cdh13 in retinal-tectal connectivity and its possible role in visual behavior circuits could possibly be applied to other CNS brain regions. In human GWAS studies, Cdh13 has been associated with a range of neuropsychiatric disorders. Mutations in Cdh13 have been associated with ADHD (Arias-Vasquez et al., 2011; Lesch et al., 2008; Mavroconstanti et al., 2014; Neale et al., 2008; Neale et al., 2010; Rivero et al., 2015; Zhou et al., 2008), drug/alcohol abuse (Edwards et al., 2012; Hart et al., 2012; Treutlein et al., 2009; Uhl et al., 2008; Yang et al., 2015), depression (Edwards et al., 2012; Sibille et al., 2009), autism (Sanders et al., 2011), schizophrenia (Borglum et al., 2014) and bipolar disorder (Xu et al., 2014). It has also been associated with personality traits such as extraversion (Terracciano et al., 2010) and violent behavior (Tiihonen et al., 2015). Understanding the role Cdh13 plays between synaptic partners in the retinal-tectal pathway may shed light on how mutations in Cdh13 in humans cause these disorders.

SUMMARY

This study explores the role of a homophilic type 2 cadherin in interneuronal anatomical maintenance. In the visual system, type 2 cadherins have been shown to direct anatomical and connectivity changes in the retina (Duan et al., 2014; Duan et al., 2018). The expansion of this work to the retinal-tectal projection pathway suggests a more general role of Type-2 cadherins in cell type-directed circuit formation in other parts of the CNS. Also, the identification of cadherin-directed circuit pairs from the retina to the SC can further the understanding of how visual inputs are relayed to inform behavioral outputs. The understanding of cadherins in maintaining these pathways can then inform on how cadherin mutations can cause various disorders as are observed in human GWAS studies.

CHAPTER 3:

FURTHER STUDIES IN CDH13 MECHANISM AND FUNCTION

INTRODUCTION:

Chapter 2 demonstrates Cdh13's role in retinal-tectal wiring. Specifically, it is necessary for maintaining mature spines in WF cells with both retinal and superior collicular Cdh13 expression needed. Building off this information, further questions were posed regarding the mechanism and function of Cdh13 in the SC region. First, does Cdh13 localize at dendritic spine heads in maintaining dendritic spines? Also, can the phenotype be rescued in adult Cdh13 knock-out mice by the viral reintroduction of Cdh13? Most importantly, do Cdh13-dependent anatomical changes result in connectivity changes? In this section, results will be presented from multiple preliminary experiments addressing these questions and expanding on related topics. In addition, supplemental information regarding Cdh13-RGC identity and possible roles for Cdh13 in RGC axonal targeting are presented. Finally, methods for future conditional knockout experiments will be discussed. The goal of this chapter is to not only provide supplemental data supporting the core thesis of this study, but to also provide experimental insight for future studies.

Chapter 3.1: Where in the world is Cadherin-13 Protein?

Identifying where Cdh13 localizes in WF is important for understanding the role of Cdh13 in retinal-tectal connectivity. Given the results of chapter 2 in this study, it is hypothesized that Cdh13 is involved in transsynaptic maintenance of dendritic spines between Cdh13-expressing cell types. Therefore, it is hypothesized that Cdh13 resides in dendritic spine heads.

The visualization of Cdh13 protein is difficult. Specific cadherin immunostaining has been notoriously difficult in the past because of the similarity in structure between cadherin family members. Although Cdh13 is unique from other type 2 cadherins given its lack of an intercellular domain in favor of a GPI anchor, its extracellular domain is similar to its relatives (Hirano & Takeichi, 2012). Similarly, Cdh6, Cdh8, and Cdh10 have proved to be difficult to stain for in our lab and have instead needed transgenic mouse lines in order to visualize their expressing populations with Cdh6-CreER, Cdh8-LacZ, and Cdh10-CreER lines. Previously reported attempts to immunostain Cdh13 were successful in chick tectum (Miskevich et al., 1998) and rat cortex (Hayano et al., 2014). However, in both cases the stains were only successful in embryonic samples. Also, the stains were concentrated at the cell membranes, as is expected of Cdh13, creating a sea of signal in which it was difficult to identify dendritic or spine structures. In these studies, it is also difficult to distinguish positive cell bodies from neighboring negative cell bodies due to how pervasive the stain was. Using the antibody used in Miskevich et al 1998, we were able to stain for Cdh13 with similar patterning to their reports in the chick tectum (Fig 3.1A). The antibody does appear to be an indicator of Cdh13 expression since this patterning is absent in Cdh13 knock out mice, (Fig 3.1A, right). Unfortunately, similar to previous reports, the high signal density made it difficult to identify coexpression with dendrites or spines. Therefore, Cdh13 antibody staining is not a practical method for localizing the protein in dendritic spines.

In the mouse, in situ hybridization labeling of Cdh13 cells is typically chosen over immunohistochemistry (Tantra et al., 2018). In chapter 2, Cdh13 expressing cells were identified using in situ hybridization, but protein localization was not possible with this method. Virally delivering a mCherry-tagged Cdh13 was hypothesized as a viable option for visualizing Cdh13 localization in the WF dendrites. A Cre-dependent AAV2-CAG-DIO-Cdh13-mCherry-WPRE was cloned by Dr. Kenichi Toma (Post-doc in our lab). This virus was injected into Cdh13-CreER-Homozygous;Thy1Stp15 SC at p1 in order to observe where Cdh13 is trafficked in the cell. mCherry-expression was observed in SC WF cells showing successful cellular uptake and expression of the fluorescent construct. However, instead of the fluorescence localizing at the cell membrane as is expected of Cdh13, the cells were filled, suggesting an issue with trafficking of the inserted construct (Fig 3.1B). Attempts to confirm Cdh13 protein expression using the Cdh13 antibody also proved unsuccessful (not shown).

Cdh13 mRNA expression can be confirmed, however, using in situ hybridization (Fig 3.1C). At p30, Cdh13 mRNA can be robustly detected only in the injected hemisphere (Fig 3.1C right). This shows that the viral construct is indeed allowing for Cdh13 mRNA transcription at the injected site. However, the Cdh13 mRNA expression pattern does not match that of the Cre-expression, visualized by YFP expression, and is restricted to WF cells in the sSC (Fig 3.1C right, green). Although the mCherry expression is restricted to GFP(+) cells, it does not correspond with the Cdh13 mRNA distribution pattern (Fig 3.1C). It is unlikely for the Cdh13 mRNA pattern to be a result of viral construct expression outside of Cre-expressing cells. Given the double-floxed open reading frame construction (DIO) of the Cdh13-mCherry construct, it is unlikely to have expression leakage. If there was leakage, mCherry expression would correspond with Cdh13-mRNA expression. Another possibility is that Cdh13-mCherry mRNA is being removed from the cell, possibly into neighboring

glia. Regardless of the reason, this method is not optimal for identifying Cdh13-protein localization within WF cells.

Determining whether Cdh13 localizes at dendritic spine heads in WF cells is important for understanding the role of Cdh13 in this system. Chapter 2's results show that Cdh13 is necessary for the maintenance of mature dendritic spines, and that this maintenance requires its expression in both the post-synaptic and pre-synaptic populations. In addition, Cdh13's GPI anchor coupling suggests that it is associated with lipid rafts, a structure often required at post-synaptic terminals at spine heads. Therefore, it is strongly hypothesized that Cdh13 would concentrate at dendritic spine heads. However, attempts to prove this hypothesis using currently available methods have not so far been successful.
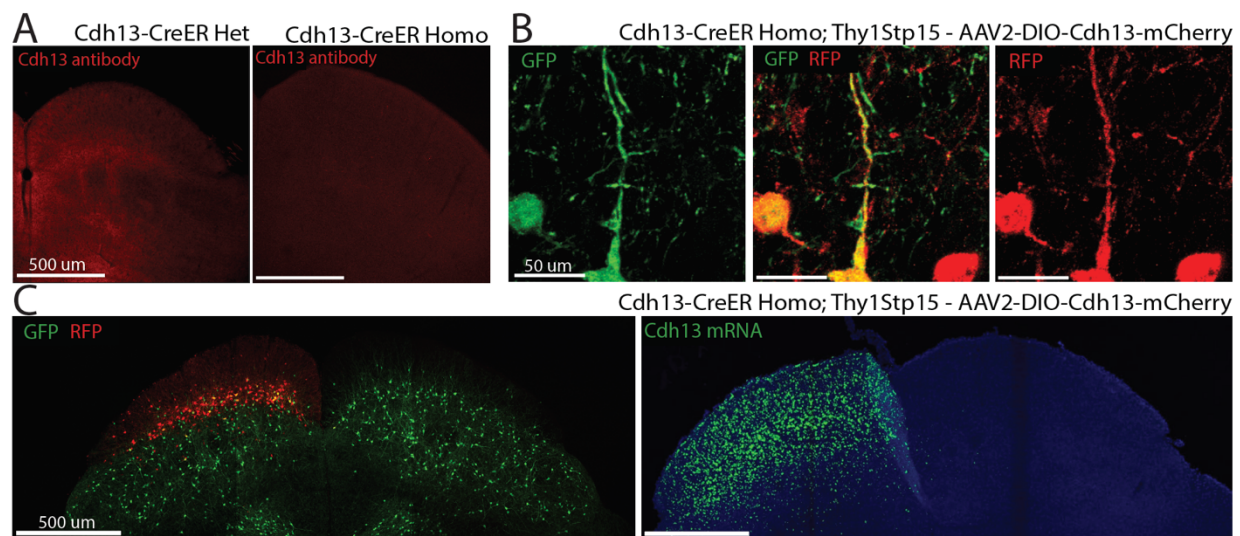
Figure 3.1 Where in the world is Cadherin 13 protein?
   (A) Confocal images of Cadherin 13 rabbit antibody signal distribution(Miskevich et al 1998) on mouse superior collicular coronal sections. (left) on Cdh13-CreER Heterozygous samples and (right) on Cdh13-CreER homozygous sample that does not have Cdh13 expression.
   (B) Confocal images of a Cdh13-CreER homozygous;Thy1stp15 labeled WF cell dendrite (green, left) filled with (yellow, center) mCherry (red, right) from injected AAV2-DIO-Cdh13-mCherry.
   (C) 10x image of the same sample presented in (B). (left) Image showing robust tamoxifen induced Cre-dependent YFP expression (green) in the SC with unilateral sSC restriction of viral mCherry expression (red). (right) Same sample shown in left after RNAScope in situ hybridization processing labeling Cdh13 mRNA (green). The Cdh13 mRNA expression is restricted to the same injected hemisphere as mCherry expression (left).

Chapter 3.2: Can Cdh13-dependent spine loss phenotype be rescued in adult mice?

Reintroduction of Cdh13 to cells that lack the protein could rescue the observed dendritic spine loss. Understanding whether Cdh13 rescue is possible in the adult would inform on its role and mechanism in spine maintenance. In the adult, if Cdh13 expression in the KO mouse rescues the spine loss phenotype, it suggests that Cdh13 is involved in initiating spine outgrowth under normal conditions.

The Cre-dependent overexpression vector was unilaterally injected into p1 Cdh13-CreER HOMO; Stp15 SC. Tamoxifen was administered at p15 as previously described in Chapter 2 for optimal Cre-induction. Overall spine density and individual spine type densities were not greater than endogenous KO samples (Fig 3.2A,B). In addition, remaining spine distribution were comparable between the two conditions (Fig 3.2C). It is therefore concluded that the phenotype was not rescued.
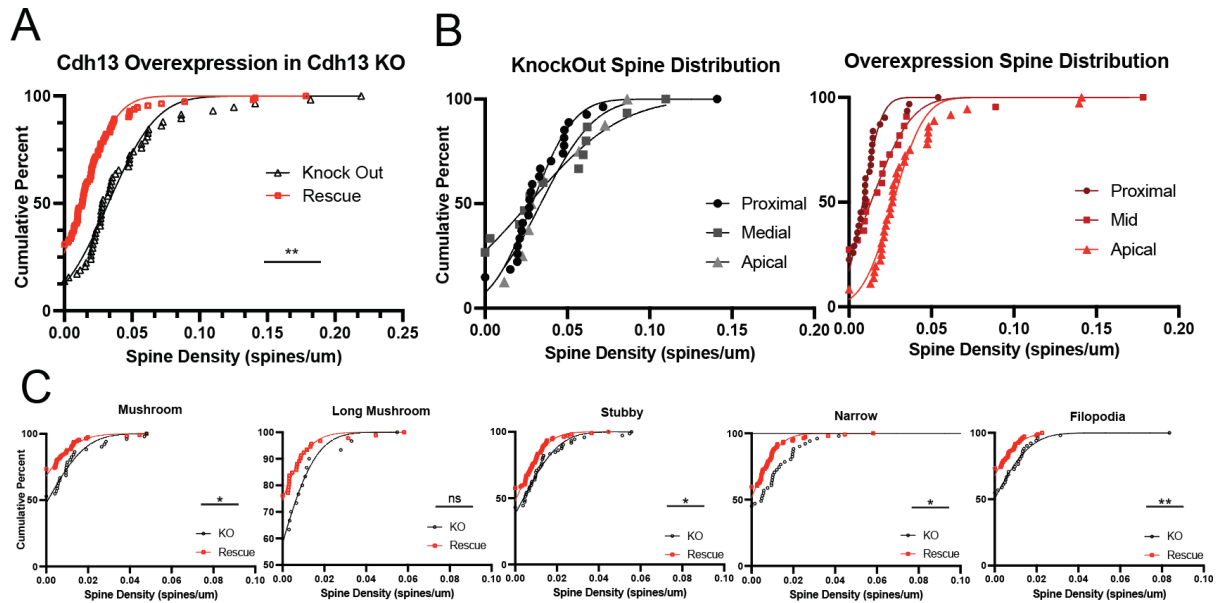
Figure 3.2 Cadherin 13 overexpression does not rescue Cdh13 KO spine loss.
(A) Cumulative percent graph comparing the populational spine densities of endogenous Cdh13 knock out, Cdh13-CreER homozygous; Thy1Stp15 YFP mice, (black), and the rescue condition (red). The rescue condition consist of the same knock out mouse injected in the SC with a Cre-dependent Cdh13 overexpression vector.
(B) Cumulative percent graphs comparing the spine distribution of the knock out (black, left) and the overexpression in the knock out (red, right).
(C) Cumulative percent graphs comparing the spine densities of each spine type in knock out and overexpression in knock out conditions.

The lack of phenotypic rescue may have occurred for a variety of reasons. Primarily, if other factors that are temporally restricted to early developmental periods are necessary for spine regrowth in the adult, Cdh13's mechanism in this process would not be applicable. Alternatively, Cdh13 expression in both the presynaptic and post-synaptic partners may be necessary for proper rescue. As shown in chapter 2, knocking down Cdh13 in either WF cells or in Cdh13-RGC both produce a similar reduction in mature spine numbers in the affected area. Therefore, Cdh13 reintroduction in both the retina and the SC may be necessary to see a phenotype rescue. Perusing this line of experimentation will shed greater light on Cdh13's mechanism in this pathway.

Embryonic and post-natal rescue would also be informative for this purpose. Although embryonic or early post-natal reintroduction of Cdh13 may allow for sufficient phenotypic rescue, viral Cre-dependent Cdh13 expression would not be possible in the Cdh13-CreER mice due to the temporal restriction of Cre-expression by tamoxifen induction. Tamoxifen induction earlier than p15, either through gavage or IP injection, at a sufficient dosage for Cre-expression in this mouse line results in death. Lower dosages result in insufficient Cre-expression. Embryonic induction by gavage feeding or IP injection of the pregnant mother also does not yield sufficient Cre-expresison in the pups in this mouse line. Regardless, because the viral expression levels would only be sufficient no earlier than a week after onset of expression, even a non-Cre-dependent construct would require an early embryonic injection. Therefore, for our current experimental protocol for Cdh13 knockout does not allow for developmental reintroduction of Cdh13.

Chapter 3.3: Is Cdh13 necessary for retinal-tectal connectivity?

Changes in synaptic connectivity often accompany changes in spine anatomy. Loss of spines is associated with a decrease in synaptic function, synaptic transmission, and has been shown to block LTP and LTD mechanisms (Boros et al., 2019; Boros et al., 2017; Okamoto et al., 2004). Given this, it is likely that knocking out Cdh13 also disrupts connectivity to WF cells. To test this hypothesis non-Cre-dependent WGA-mCherry (AAV2-WGA-mCherry) was injected into Cdh13-CreER heterozygous and homozygous adult retina. Because the virus expression is not Cre-dependent, the starting population will not consist of a specific cell type. Given the magnitude of mature spine loss in WF cells due to Cdh13 knock out, it is hypothesized that general glutamatergic input is decreased. Therefore, regardless of the starting population, the goal of the experiment is to detect a decrease in the number of WGAmCherry (+) WF cells. 2 weeks after injection, retina and SC samples were fixed and collected. Unfortunately, tamoxifen induction of Cre expression was unsuccessful for both groups so direct count of WGA(+) WF cells was not possible. However, laminar boundary analysis (Chapter 1.1) can be used to determine changes to WF retinal input, which, together with changes in resulting WGA-mCherry content in the cell bodies, would cause lower relative fluorescence in the lower SO. Because WF cell bodies reside in the lower SO and the lower SO has relatively low RGC axonal innervation (Fig. 1.1F) changes in WF cell WGA-mCherry transfer are more easily detectable.

When comparing the fluorescence patterns of control and knockout WGA transfer, there is not a significant difference between the two distributions (Fig 3.3). This may indicate that there is no change in connectivity between the retina and WF cells. This result may also be a result of other SO and SGI retinal-recipient neurons whose WGA-mCherry signal obscures any decrease to WF cells. This is likely given previous evidence (Fig 2C, D) showing many retinal recipient neurons deeper than RGC axonal lamina. However, it may be possible that only Cdh13 input is affected by removal of Cdh13, therefore WF cells may still receive signal from non-Cdh13 expression RGCs.

To test whether connectivity between Cdh13 expressing populations would be affected due to knocking out Cdh13, Cre-dependent viral WGA-mCherry in Cdh13-CreER;Thy1Stp15 mice was used to detect changes in connectivity between Cdh13-RGC and Cdh13-WF cells. The advantage of using this line is that it allows for Cdh13-cell Cre-labeling with or without Cdh13 expression. In Cdh13-CreER heterozygous control and homozygous knockout mice, AAV2-Dio-WGA-mCherry was injected into the eye at p1. Tamoxifen was administered at p15 as previously described. At p30, retinal and SC tissue was fixed, collected, and analyzed. The goal was to target Cdh13-RGC as the starting population then compare the number of Cre-expressing cells in the SC that receive WGA-mCherry through transsynaptic transport. This would allow for a comparison of changes in connectivity between Cdh13 RGC and Cdh13 SC cells between control and knockout conditions.

Unfortunately, the Cre-dependent WGA would not express in the retina in these mice. In all injected retina (n = 12 mice, 24 eyes), not a single retinal cell was mCherry+. This is in direct contrast to the infection efficiency of the same virus in other mouse lines such as KCNG-Cre Tsai (Tsai et al., 2022). This consistent lack of infection in the Cdh13-CreER line is likely because of the temporal restriction because it needs tamoxifen induction for proper Cre function. The same issue occurred in other CreER mouse lines in the lab including Cdh6-CreER, Cdh10-CreER, and Cdh6910-CreER mice. Cre-dependent WGA transsynaptic tracing for labeling and single cell mRNA sequencing was attempted in each of these lines, but ultimately failed due to low starting population infection rates in the retina. So, although the Cdh13-CreER has a much greater tamoxifen-induced Cre expression rate compared to the other lines, it is consistent that the lab's Cre-dependent WGA system does not work in Cdh13-CreER mice.

Another notable observation is the lack of Cre-expressing RGCs regardless of viral infection. Since the Cdh13-CreER mice have the Thy1-STP15 gene, any cell that expresses Cre should be YFP(+). If there is an issue with expression of WGA-mCherry Cre due to Cre-expression levels, there

should still be the same number of YFP(+) RGCs as un-injected retina. However, very few YFP(+) RGCs are observed in these retina. The few that are observed are also RFP(-). Although the Cre-induction rate in the retina of Cdh13-CreER mice is already consistently low in both the heterozygous and homozygous (n = 10-15 cells per retina in both conditions, 10 mice sampled), the number of GFP(+) RGCs was significantly lower (3 GFP(+) neurons total for all samples). This was especially surprising given that Cre expression was robust in the SC of these samples. There may be some cellular toxicity from WGA-mCherry expression causing cell death in infected cells. It is unclear whether this toxicity is higher in certain RGC cell types or whether it is an overall percentage that is negligible with higher expression rates but is more noticeable given the smaller sample size observed here. Nevertheless, the inability to express WGA-mCherry in the Cdh13-RGC population makes this line impractical for determining changes in connectivity from this population.

Retrograde transsynaptic tracing from WF cells is a viable option for future study. WF cells have more options for genetic access than Cdh13-RGCs, so more experimental configurations can be used to target them as the starting population. In addition, WF cells robustly express Cre in Cdh13-CreER mice. Therefore, using a G-deleted rabies with Cre-dependent TVA+G system to specify starting population in the Cdh13-CreER mouse would be a viable option for determine changes in connectivity between these two populations. This would also allow for Cdh13-RGC identification since there would be no WGA-mCherry induced cell death. Genetic labeling of Cdh13-RGC is the most viable method of labeling because Cdh13 mRNA cell labeling is only available in control conditions with Cdh13 expression, not in the knockout conditions. Labeling the subpopulations of Cdh13-RGC is also not an option because large portions of each population may not express Cdh13. Alternatively, using an NPNT flp; Cdh13 CreER; Thy1Stp15YFP mouse would allow flp-dependent targeting of WF cells for transsynaptic retrograde rabies tracing onto Cdh13-CreER;Thy1StpYFP labeled RGC. There are many experimental possibilities for determining Cdh13-dependent changes in connectivity.
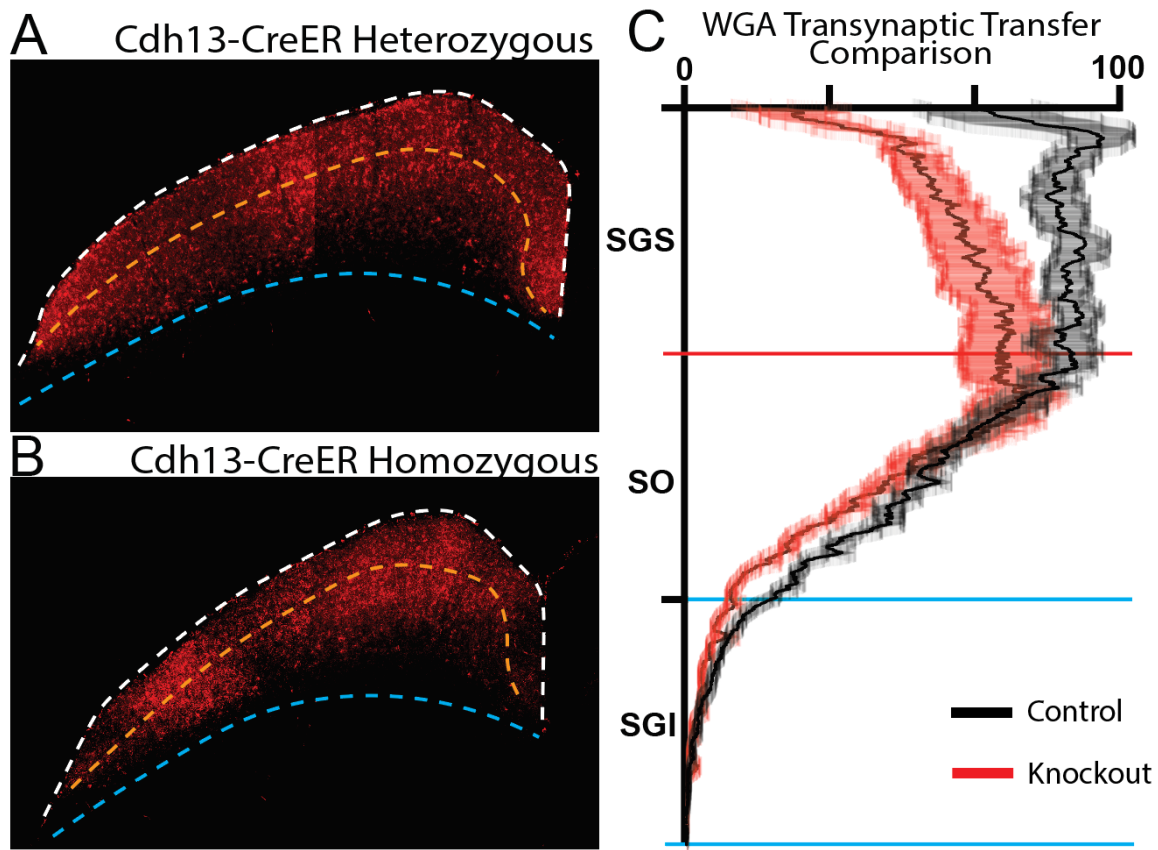
Figure 3.3 Laminar boundary fluorescence analysis of transsynaptic WGA transfer under Cdh13 KO

(A) Confocal image of SC hemisphere contralateral to the AAV2-WGA-mCherry injected eye of the control Cdh13-CreER heterozygous mouse. Laminar boundaries are defined by lines representing the immunohistochemical boundaries (not shown) as defined in figure 1.1. The MBP boundary between the SGS and the SO is yellow instead of red for visibility. The red fluorescence is WGA-mCherry stained with RFP-rbt.

(B) Confocal image image of the contralateral SC hemisphere to the injected eye under the same experimental, analytical, and display conditions as (A) under Cdh13 KO conditions in the Cdh13-CreER homozygous mouse.

(C) Laminar boundary analysis (method described in Chapter 1.1) comparing the WGA-mCherry distribution in the control and Cdh13-KO.

Chapter 3.4: Does Cdh13 affect RGC axonal targeting in the SC?

In rat cortical development, Cdh13 was shown to direct axonal path finding (Hayano et al., 2014). This precedent suggests the possibility that knocking out Cdh13 would affect Cdh13-RGC axonal lamination. Cdh13-RGC axons are restricted to the SGS, while SO-terminating RGCs, such as aRGCs, do not express Cdh13. It is therefore hypothesized that Cdh13 could be involved in SGS laminar targeting for RGC axons, where knocking out Cdh13 would result in SO lamination, and ectopic expression would result in SGS lamination.

Axonal lamination was therefore compared between heterozygous control mice and homozygous knockout Cdh13-CreER mice. In order to isolate the axonal labeling in the SC from Cdh13-WF labeling, Cdh13-CreER mice without the Thy1-Stp15 gene were used. Their eyes were injected intravitreally with a Cre-dependent GFP to label Cdh13-RGC at p0. Two weeks after p15 tamoxifen induction, samples were fixed and collected. No laminar differences were detected between heterozygous and homozygous knockout conditions (Fig 3.4A). It was therefore concluded that Cdh13 knockout does not affect Cdh13-RGC axonal laminar targeting in the SC, as hypothesized above.

The possibility that ectopic Cdh13 could be able to drive axons to the SGS was then tested. AAV2-DIO-Cdh13-mCherry overexpression vector was injected into p0 eyes of KCNG-Cre mice to ectopically express Cdh13 in aRGCs. No change in axonal lamination was observed (Fig 3.4B top right). Given the combination of results showing neither Cdh13 KO nor Cdh13 ectopic expression changing RGC axonal targeting in the SC, Cdh13 is unlikely to be a determinate of axonal lamination in retinal-tectal projections.

This experimental system was also used to determine whether the Cdh13 protein localizes at presynaptic terminals. To determine this, the Cdh13-overexpression virus was co-injected with a AAV2-DIO-synaptophysin-eGFP into p60 adult KCNG-Cre eyes. Synaptophysin is a presynaptic

protein, therefore co-expression of Cdh13-mCherry with Synaptophysin-GFP would suggest the concentration of Cdh13 at presynaptic terminals. Upon infection, the Cdh13-mCherry filled the axons, similar to their expression in the SC (Fig. 3.1B), so co-expression with punctated synaptophysin-GFP does not indicate localization of Cdh13 at presynaptic terminals.

At this point it was made known by the creator of the mouse line that the genetic composition of the KCNG-Cre mouse line is not as previously described. Although the line consistently labeled aRGC in the retina, it was previously unpublished that the line is a knock-in/knock-out Cre line. This means that the insertion of Cre behind the KCNG promoter disrupts KCNG expression. Therefore, the homozygous mouse is a full endogenous knock-out for the potassium channel, KCNG.

In addition, it was made known that in the homozygous mouse, the aRGC axons have been observed but have not been published to extend into the SGS, as was observed in the double over-expression experiment. Using the laminar boundary analysis method developed in this thesis (Chapter 1.1), the laminar shift into the SGS is quantifiable and significant (Figure 3.4C) (n=3 mice). Synaptophysin-GFP expression alone in heterozygous KCNG-Cre aRGCs did not induce a laminar shift (n = 5 mice). Although the possible conclusions from the observed laminar change are confounded by the knockout of KCNG, the analysis methods developed and used in this thesis proved effective in quantifying the laminar change observed.

Regardless of the mechanism, a laminar shift in axonal targeting in the SC is an interesting phenomenon since it could have large implications for connectivity and visual behavior. Determining KCNG function and mechanism in axonal targeting would have significant applications for developmental and clinical studies. aRGCs, labeled by KCNG-Cre, are more resilient to glaucoma related apoptosis (Duan et al., 2015). Exploring the role KCNG has in this phenomenon is an interesting avenue to pursue.
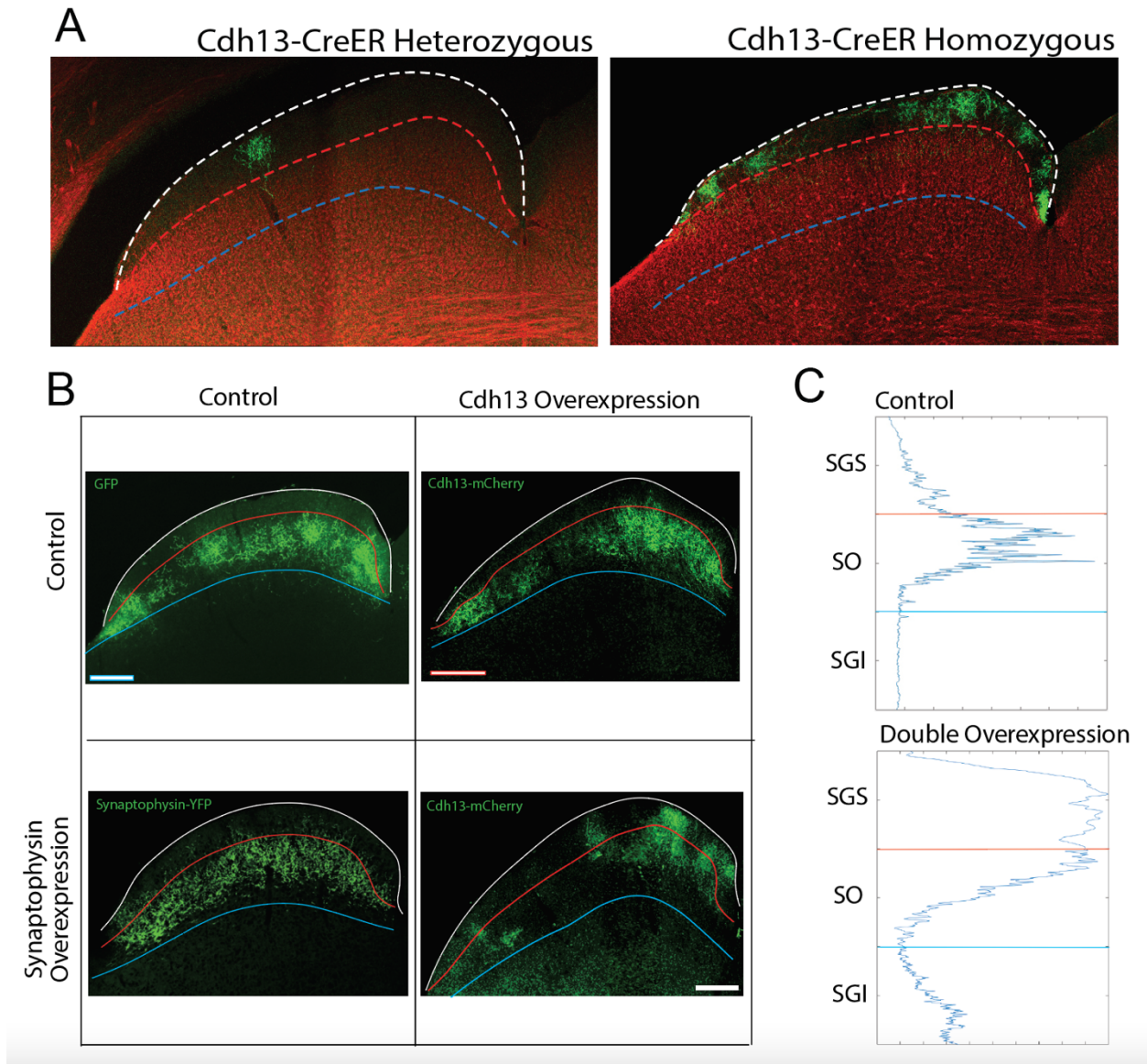
Figure 3.4 Cadherin-13 does not affect RGC laminar targeting, while KCNG homozygous mouse has altered axonal lamination.

(A) Confocal images comparing Cdh13-RGC axonal lamination under control and Cdh13 KO conditions (green). Lamina are noted by colored lines as defined in Figure 1.1.

(B) Confocal images comparing aRGC lamination under different over-expression conditions. (top left) Control: AAV2-DIO-GFP p30 retinal injection. (top right) Cdh13 ectopic expression: AAV2-DIO-Cdh13-mCherry p0 retinal injection, (bottom left) Synaptophysin overexpression: AAV2-DIO-Syn-GFP p30 retinal injection, (bottom right) double overexpression: p60 retinal injection. Whether the mice were heterozygous or homozygous for KCNG-Cre is unclear.

(C) Laminar boundary analysis comparison of aRGC axon control lamination and double overexpression lamination.

Chapter 3.5: Conditional Cdh13 KO provides optimized experimental parameters

Three critical components for appropriate determination of Cdh13 knockout phenotype are (1) temporal control (2) spatial control and (3) labeling of Cdh13-expressing cells. The Cdh13-CreER line allows for appropriate cellular labeling, but it lacks temporal or special control of Cdh13 knockout. Using a virally-mediated shRNA knockdown of Cdh13 allows for spatially specific infection and some temporal control. When used in conjunction with a WF cell-labeling mouse line, such as NTSR1-GN209 or Cdh13-CreER, this system has all three components. However, shRNA targeting is not an optimal method as it can have incomplete knockdown or off-target effects. A more optimal experimental tool is the use of a conditional knockout system.

Using a conditional Cdh13 mouse line (Poliak et al., 2016), Cdh13 knockout can be achieved locally and in a temporally controlled manner. For example, injection of AAV-Cre into the retina will knock out Cdh13 exclusively in the retina (Fig 3.6A). One drawback of this line is the lack of cell type-specific labeling. Cdh13-expressing cells cannot be specifically labeled genetically, and after Cdh13 knockout, Cdh13 mRNA staining will not label the endogenously Cdh13 expressing cells. So even though co-injection with a Cre-dependent fluorescent marker or Cre immunolabeling will label the affected population, the Cdh13-expressing population cannot be isolated. Nevertheless, for the purposes of knocking out Cdh13 in all Cdh13-expressing RGC, this method is applicable.

An issue arises when trying to label Cdh13-expressing WF cells. One possibility is to use a Cdh13cKO crossed with NTSR1-GN201-Cre, allowing for WF cell labeling, since over 90% over NTSR1-WF cells are Cdh13 expressing (Fig. 2.3). However, using a Cre line to label cells in the SC removes the conditional knockout specificity to the retina, since WF cells labeled by Cre will also have Cdh13 knocked out. In addition, many RGCs express Cre in NTSR1-GN209-Cre retina (Fig. 2.7D), so knockout is not restricted to WF cells either. A similar issue occurs when using Cdh13-CreER heterozygous mice for the same purpose. When Cre expression is induced in the SC and the retina,

Cdh13 is knocked out in those cells. Neither of these WF cell-labeling lines allow for spatial restriction of Cdh13 knockout.

Another option is to indiscriminately label SC cells with a low titer virus. This would ideally label some WF cells that can then be manually identified. However, WF cell anatomy may allow for a more efficient design. WF cells primarily project to the lateral posterior nucleus (LP) of the thalamus (LP). Of sSC cell types, they are the only cell type to project to this region (Gale & Murphy, 2014, 2018). One method to label WF cells without Cre is to take advantage of this concentrated projection. Theoretically, axonal uptake and subsequent retrograde fluorescent labeling by viral injection into the LP would specifically label WF cells without the need for Cre. This would allow for exclusive Cre expression and Cdh13 knock out in the retina through viral injection. Figure 3.6A illustrates the injection plan. 200uL of AAV5-mGFP was injected unilaterally into the LP to test this method. LP is a small nucleus and in practice, is difficult to isolate an injection within its boundaries without bleeding into neighboring structures. One neighboring structure, the dorsal lateral geniculate nucleus (DLGN), also receives input from the sSC. Therefore, viral infection in this area may label non-WF cells. Despite non-WF cells being labeled, more WF cells are labeled (Fig 3.6C, left) than in direct SC injections (not shown). Unfortunately, the retrograde labeling was successful in labeling the cell bodies of WF cells, but they did not sufficiently label WF dendrites or spines for analysis (Figure 3.6 right). It may be possible that a different retrograde viral construct would be able to appropriately label WF cells for spine analysis, but currently this method does not seem to be practical for the purpose.

A promising method in development is the use of Cdh13 cKO; NPNT flp mice. The NPNT flp line (Tsai et al., 2022) will allow for flp-dependent labeling of WF cells, allowing exclusive Cre expression in the retina via injection. By injecting a flp-dependent GFP into the SC at p0, AAV9Cre+AAV9-Dio-tdTom can be injected into the eye at specific time points. This method will allow for (1) temporal control by deciding when to inject Cre, (2) spatial control by deciding where to

inject the Cre and (3) have WF cell-specific labeling to analyze the effect Cdh13 conditional knock out

has on its dendritic spines. In addition, the conditional knockout allows for a complete removal of

Cdh13 expression.
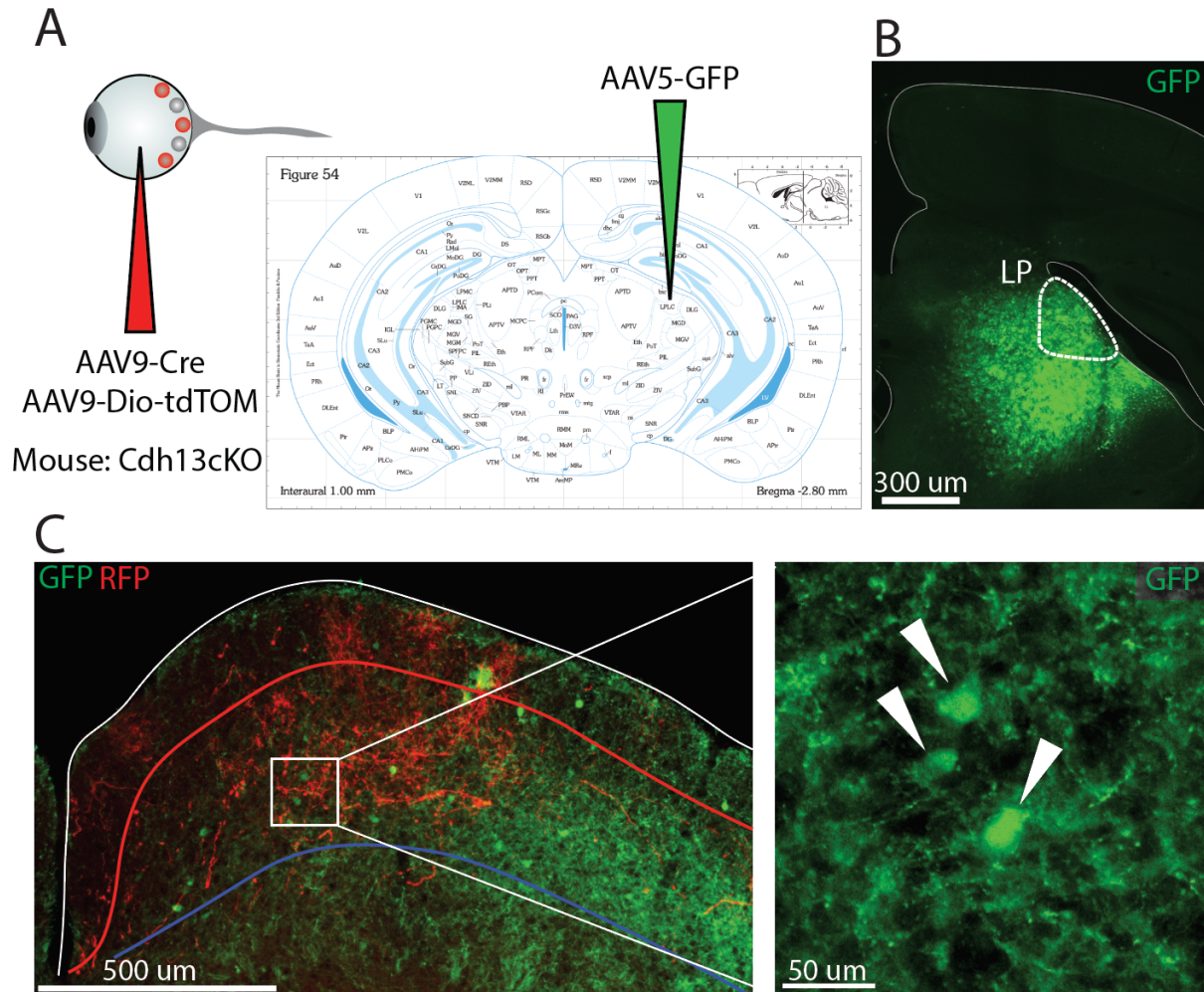
Figure 3.5 Experimental design for restricted conditional knockout
- (A) Cartoon schematic of injection plan to label WF cells via LP injection with a fluorescent reporter and knock out Cdh13 exclusively in the retina by injected Cre and a fluorescent reporter.
- (B) Confocal image of LP injection targeting with AAV5-GFP
- (C) Confocal image of SC in same animal in (B). Cells retrogradely labeled by the injection in (B) are labeled in green. Cre-expressing axons are labeled in red. Higher magnification image (right) shows AAV5-GFP labeled cell bodies. White arrows mark labeled WF cell bodies.

SUMMARY

Chapter 3 presents exploratory methods and data addressing further questions on Cdh13's role in the superior colliculus. Understanding where Cdh13 protein is localized (Chapter 3.1) and whether its role in spine anatomy also affects connectivity (Chapter 3.3) are important next steps in understanding its mechanism of action. Although the results are preliminary, they provide practical validation of the methods established in Chapter 1 of this thesis (Chapter 3.3, 3.4) and test genetic tools for further manipulation of Cdh13 expression (Chapter 3.1, 3.2, 3.5). This provides an important foundation for future studies.

Concluding thoughts

The ability of neurons to form synapses with appropriate partner cells is essential for CNS function. The central goal of this thesis is to begin to map cadherin expression and mechanisms governing cell type-specific synaptic choice. Using the retinal projection to the superior colliculus as a model system, this thesis identifies cadherin 13 in wide field cells and its role in maintaining mature dendritic spines in this population. Although previous studies have established cadherin pairs/groups that direct anatomy and connectivity in the retina (Duan et al., 2014; Duan et al., 2018), the work presented here translates these principles to the brain. In Chapter 2, both retinal and SC Cdh13 is shown to be necessary in maintaining mature spine anatomy in wide field dendrites.

Cadherin 13 is one of many cadherins expressed in the superior colliculus and investigating other cadherin-expressing population pairs will enhance our understanding of molecular determinants in circuit development. To facilitate this, the methods and results established here can guide future studies. Consistent laminar analysis of dendrites, axons, and transsynaptic tracers is critical for assessing cadherin-dependent changes in this system and Chapter 1 provides novel methods for achieving this. In addition, the preliminary results and exploratory experimental designs of Chapter 3 provide an experimental basis to build upon. Identifying more molecules directing cell type-specific connectivity and understanding their mechanisms would allow for greater behavioral understanding and clinical applications. And I hope that this study can contribute towards that goal.

Materials and Methods

Mice

All animal experiments were approved by the Institutional Animal Care and Use Committees at the University of California, San Francisco (UCSF). Mice were maintained under regular housing conditions with standard access to drink and food in a pathogen-free facility. Male and female mice were used in equal numbers and no sexual dimorphisms were observed.

- Gad2-Cre, Rorb-Cre, *Ntsr1-GN209*-Cre and *Grp-KH288*-Cre were previously used to label horizontal, stellate, wide-field and narrow-field neurons in the SC Gale (Gale & Murphy, 2018). *Ntsr1-GN209-Cre* and *Grp-KH288-Cre* were generous gifts of Charles Gerfen (National Institute of Mental Health).

- Cdh13-CreER mouse line has estrogen receptor conjugated Cre gene inserted into the Cdh13 gene behind the Cdh13 promoter. This allows for CreER expression in Cdh13 expressing cells while disrupting Cre Expression in that allele. Previously published in (Poliak et al 2016)

- Thy1-stop-YFP Line #15 transgenic mice express EYFP driven by Cre recombinase in many neuronal populations, including most RGCs and projection neurons in the brain and spinal cord. We crossed this line with the SC neuron-marking Cre driver lines and Cdh13-CreER line listed above to visualize neuronal morphology. (Buffelli et al., 2003)

Tamoxifen Administration

Tamoxifen was injected interperitoneally (20mg/mL, 100uL per dose) at p13, p15, and p17 for a total of 3 doses. Humane euthenization through transcardial perfusion (see histology) was performed at p30, approximately 2 weeks after the initial tamoxifen dose.

Neonatal Injections

Neonatal superior collicular injections were performed at ages p0-2, when the lambdoid suture and collicular hemispheres are still visible through the skin. The mouse is anaesthetized on ice in accordance with protocols. The viral injection is made with a pulled glass pipette through the skin and the skull (volume 0.33 uL per hemisphere). Saline control was injected in the opposite hemisphere. Mouse was returned to cage after warmed and alert. Tissue was collected and mouse was euthanized (see histology) at p30.

Adult Intercranial Injections

Mice were anesthetized with continuous 2% isoflurane/Oxygen on a stereotax (Model 940, David Kopf Instruments). Meloxicam (5mg/kg) was administered IP before the surgery and 1 day after surgery. Viruses were loaded into a pulled glass pipette connected with a syringe (7634-O, Hamilton) by a dual ferrule adaptor (55750-0, Hamilton). Injection speed and volume were controlled by a Microinjection Syringe pump (UMP3T-1, WPI). AAV2-Ef1a-shCdh13-2A-mCherry was injected into the right hemisphere of p60 NTSR1-GN209-Cre mice. Coordinates: 3.6 mm posterior and 0.7 mm lateral to bregma and 1.0 mm below the skull. Volume: 300nL. Four weeks later the mouse was humanely euthanized via transcardial perfusion (see histology). Brain and retinas were collected for immunohistochemical analysis.

Interocular Injections

Intraocular injection of AAVs was performed as previously described (Duan et al., 2015; Hong et al., 2011)

For Cdh13 RGC axonal tracing experiment, p1 Cdh13-CreER mice were injected uni-ocularly with 0.5uL AAV5-DIO-GFP using a sharpened glass pipette.

For retinal Cdh13 knockdown experiment, p60 NTSR1-GN209-Cre was injected with 1uL AAV2-ef1a-shCdh13-2A-DIO-mCherry in the right eye. 4 weeks later, the mouse was humanely euthanized and transcardially perfused. Brain and retinal tissues were collected (see histology).

Viral Production

To make pAAV-hU6-shCdh13-DIO-mOrange2 for Cdh13 LOF studies, hU6-shCdh13 cassettes were generated using the following long primers with Mlu1 site from (pXX). These cassettes were cloned to the Mlu1 site of pAAV-DIO-mOrange2. pAAV-DIO-mOrange2, a backbone of shRNA plasmid, was modified from pAAV-Ef1a-DIO-ChR2-EYFP (addgene #35507), replacing the ChR2-EYRP to mOrange2. The target sequences were adopted from Killen et al. (2017).

hU6-common-Fw: 5-AATTGAACGCGTGGGCAGGAAGAGGGC-3'

shCdh13-1-Rv: 5'-cgatacACGCGTaaaaaagGCAACGAGAAGCTGCACTAcaagcttcTAGTGCAGCTTCTCGTTGCcGGATCCtcgtcctttccac-3'

shCdh13-Rv: 5'-

cgatacACGCGTaaaaaagGCTCCTTGCAGGATATCTTcaagcttcAAGATATCCTGCAAGGAGCc

GGATCCtcgtcctttccac-3'

Histology

Tissue Collection:

Animals were anesthetized then transcardially perfused with ice cold 0.1M phosphate buffer then ice cold 4% PFA in 0.1M phosphate buffer, pH 7.4. Whole brain and eyes were collected where applicable. Dissected brain tissue was then post-fixed in the PFA solution overnight at 4C, then cryoprotected in 30% sucrose 0.2% sodium azide until they sank. The brain samples have the option to be stored at this step. Dissected eyes were placed in 4%PFA for 30 minutes on ice. Cornea and lens were then removed before a second 30 minute incubation period in 4% PFA on ice. Eye samples were then stored in 0.1M PBS 0.2% sodium azide or immediately further processed (see below).

Brain:

After sucrose cryoprotection, brains were frozen with dry ice on a sliding microtome (Leica). Floating 40um sections were collected and stored in 0.1M PBS with 0.2% sodium azide at 4C. These sections then underwent immunuhistochemical staining, in situ hybridization staining, or both.

For immunostaining, floating sections were incubated in blocking buffer (0.5% Triton X-100, 5% natural donkey serum, 0.1M PBS) at RT for 1 hour, then primary antibodies in blocking buffer overnight at 4C, then secondary antibodies in blocking buffer at RT for 2 hours. Slices were then mounted on non-polarized glass slides with vectasheild with DAPI (VectorLabs H-1200).

In situ hybridization was performed using RNAscope Fluorescent Multiplex Kit (Advanced Cell Diagnostics) following the manufacturer's instructions. Floating 40um sections were mounted on polarized glass slides for this protocol. Where applicable, samples were then immunostained using the protocol previously described before cover-slipping. Slides were mounted using vectasheild with DAPI (VectorLabs H-1200).

Retina:

Retinas were dissected from the remaining eye sample stored in 0.1M PBS, 0.2% sodium azide.

For whole mount immunohistochemistry, retina is incubated in blocking buffer overnight at 4C. Sample is incubated for 3 nights in 4C in primary antibodies in blocking buffer. After washing in 0.1M PBS, sample is incubated overnight at 4C in secondary antibodies in blocking buffer. Sample is then washed in PBS before mounting on filter paper and vectasheild with DAPI (VectorLabs H-1200) and cover slipped.

Retinas for slice immunostaining or in situ hybridization were cryoprotected in 30% sucrose for 60 minutes on ice or until it sinks. It is then frozen in OCT (Tissue-Tek) in a block. The sample is cryostat sectioned at 20um and directly mounted on polarized glass slides. Mounted tissue was either stored at -20C or directly stained (see brain protocol above).

REFERENCES

Alvarez, V. A., Ridenour, D. A., & Sabatini, B. L. (2007). Distinct structural and ionotropic roles of NMDA receptors in controlling spine and synapse stability. *J Neurosci*, *27*(28), 7365-7376. https://doi.org/10.1523/JNEUROSCI.0956-07.2007

Arias-Vasquez, A., Altink, M. E., Rommelse, N. N., Slaats-Willemse, D. I., Buschgens, C. J., Fliers, E. A., Faraone, S. V., Sergeant, J. A., Oosterlaan, J., Franke, B., & Buitelaar, J. K. (2011). CDH13 is associated with working memory performance in attention deficit/hyperactivity disorder. *Genes Brain Behav*, *10*(8), 844-851. https://doi.org/10.1111/j.1601-183X.2011.00724.x

Babb, S. G., Kotradi, S. M., Shah, B., Chiappini-Williamson, C., Bell, L. N., Schmeiser, G., Chen, E., Liu, Q., & Marrs, J. A. (2005). Zebrafish R-cadherin (Cdh4) controls visual system development and differentiation. *Dev Dyn*, *233*(3), 930-945. https://doi.org/10.1002/dvdy.20431

Basbaum, A. I., & Menetrey, D. (1987). Wheat germ agglutinin-apoHRP gold: a new retrograde tracer for light- and electron-microscopic single- and double-label studies. *J Comp Neurol*, *261*(2), 306-318. https://doi.org/10.1002/cne.902610211

Benson, D. L., & Tanaka, H. (1998). N-cadherin redistribution during synaptogenesis in hippocampal neurons. *J Neurosci*, *18*(17), 6892-6904. https://www.ncbi.nlm.nih.gov/pubmed/9712659

Borglum, A. D., Demontis, D., Grove, J., Pallesen, J., Hollegaard, M. V., Pedersen, C. B., Hedemand, A., Mattheisen, M., investigators, G., Uitterlinden, A., Nyegaard, M., Orntoft, T., Wiuf, C., Didriksen, M., Nordentoft, M., Nothen, M. M., Rietschel, M., Ophoff, R. A., Cichon, S., . . . Mors, O. (2014). Genome-wide study of association and interaction with

maternal cytomegalovirus infection suggests new schizophrenia loci. *Mol Psychiatry*, *19*(3), 325-333. https://doi.org/10.1038/mp.2013.2

Boros, B. D., Greathouse, K. M., Gearing, M., & Herskowitz, J. H. (2019). Dendritic spine remodeling accompanies Alzheimer's disease pathology and genetic susceptibility in cognitively normal aging. *Neurobiol Aging*, *73*, 92-103. https://doi.org/10.1016/j.neurobiolaging.2018.09.003

Boros, B. D., Greathouse, K. M., Gentry, E. G., Curtis, K. A., Birchall, E. L., Gearing, M., & Herskowitz, J. H. (2017). Dendritic spines provide cognitive resilience against Alzheimer's disease. *Ann Neurol*, *82*(4), 602-614. https://doi.org/10.1002/ana.25049

Bozdagi, O., Shan, W., Tanaka, H., Benson, D. L., & Huntley, G. W. (2000). Increasing numbers of synaptic puncta during late-phase LTP: N-cadherin is synthesized, recruited to synaptic sites, and required for potentiation. *Neuron*, *28*(1), 245-259. https://doi.org/10.1016/s0896-6273(00)00100-8

Buffelli, M., Burgess, R. W., Feng, G., Lobe, C. G., Lichtman, J. W., & Sanes, J. R. (2003). Genetic evidence that relative synaptic efficacy biases the outcome of synaptic competition. *Nature*, *424*(6947), 430-434. https://doi.org/10.1038/nature01844

Byun, H., Kwon, S., Ahn, H. J., Liu, H., Forrest, D., Demb, J. B., & Kim, I. J. (2016). Molecular features distinguish ten neuronal types in the mouse superficial superior colliculus. *J Comp Neurol*, *524*(11), 2300-2321. https://doi.org/10.1002/cne.23952

Ciatto, C., Bahna, F., Zampieri, N., VanSteenhouse, H. C., Katsamba, P. S., Ahlsen, G., Harrison, O. J., Brasch, J., Jin, X., Posy, S., Vendome, J., Ranscht, B., Jessell, T. M., Honig, B., & Shapiro, L. (2010). T-cadherin structures reveal a novel adhesive binding mechanism. *Nat Struct Mol Biol*, *17*(3), 339-347. https://doi.org/10.1038/nsmb.1781

Dhande, O. S., & Huberman, A. D. (2014). Retinal ganglion cell maps in the brain: implications for visual processing. *Curr Opin Neurobiol*, *24*(1), 133-142. https://doi.org/10.1016/j.conb.2013.08.006

Duan, X., Krishnaswamy, A., De la Huerta, I., & Sanes, J. R. (2014). Type II cadherins guide assembly of a direction-selective retinal circuit. *Cell*, *158*(4), 793-807. https://doi.org/10.1016/j.cell.2014.06.047

Duan, X., Krishnaswamy, A., Laboulaye, M. A., Liu, J., Peng, Y. R., Yamagata, M., Toma, K., & Sanes, J. R. (2018). Cadherin Combinations Recruit Dendrites of Distinct Retinal Neurons to a Shared Interneuronal Scaffold. *Neuron*, *99*(6), 1145-1154 e1146. https://doi.org/10.1016/j.neuron.2018.08.019

Duan, X., Qiao, M., Bei, F., Kim, I. J., He, Z., & Sanes, J. R. (2015). Subtype-specific regeneration of retinal ganglion cells following axotomy: effects of osteopontin and mTOR signaling. *Neuron*, *85*(6), 1244-1256. https://doi.org/10.1016/j.neuron.2015.02.017

Edwards, A. C., Aliev, F., Bierut, L. J., Bucholz, K. K., Edenberg, H., Hesselbrock, V., Kramer, J., Kuperman, S., Nurnberger, J. I., Jr., Schuckit, M. A., Porjesz, B., & Dick, D. M. (2012). Genome-wide association study of comorbid depressive syndrome and alcohol dependence. *Psychiatr Genet*, *22*(1), 31-41. https://doi.org/10.1097/YPG.0b013e32834acd07

Fannon, A. M., & Colman, D. R. (1996). A model for central synaptic junctional complex formation based on the differential adhesive specificities of the cadherins. *Neuron*, *17*(3), 423-434. https://doi.org/10.1016/s0896-6273(00)80175-0

Fiala, J. C., Feinberg, M., Popov, V., & Harris, K. M. (1998). Synaptogenesis via dendritic filopodia in developing hippocampal area CA1. *J Neurosci*, *18*(21), 8900-8911. https://www.ncbi.nlm.nih.gov/pubmed/9786995

Gale, S. D., & Murphy, G. J. (2014). Distinct representation and distribution of visual information

    by specific cell types in mouse superficial superior colliculus. *J Neurosci*, *34*(40), 13458-13471.

    https://doi.org/10.1523/JNEUROSCI.2768-14.2014

Gale, S. D., & Murphy, G. J. (2018). Distinct cell types in the superficial superior colliculus project

    to the dorsal lateral geniculate and lateral posterior thalamic nuclei. *J Neurophysiol*, *120*(3),

    1286-1292. https://doi.org/10.1152/jn.00248.2018

Ghosh, K. K., Bujan, S., Haverkamp, S., Feigenspan, A., & Wassle, H. (2004). Types of bipolar cells

    in the mouse retina. *J Comp Neurol*, *469*(1), 70-82. https://doi.org/10.1002/cne.10985

Gipson, C. D., & Olive, M. F. (2017). Structural and functional plasticity of dendritic spines - root or

    result of behavior? *Genes Brain Behav*, *16*(1), 101-117. https://doi.org/10.1111/gbb.12324

Grutzendler, J., Kasthuri, N., & Gan, W. B. (2002). Long-term dendritic spine stability in the adult

    cortex. *Nature*, *420*(6917), 812-816. https://doi.org/10.1038/nature01276

Hart, A. B., Engelhardt, B. E., Wardle, M. C., Sokoloff, G., Stephens, M., de Wit, H., & Palmer, A.

    A. (2012). Genome-wide association study of d-amphetamine response in healthy volunteers

    identifies putative associations, including cadherin 13 (CDH13). *PLoS One*, *7*(8), e42646.

    https://doi.org/10.1371/journal.pone.0042646

Hayano, Y., Zhao, H., Kobayashi, H., Takeuchi, K., Norioka, S., & Yamamoto, N. (2014). The role

    of T-cadherin in axonal pathway formation in neocortical circuits. *Development*, *141*(24), 4784-

    4793. https://doi.org/10.1242/dev.108290

Hayashi, Y., & Majewska, A. K. (2005). Dendritic spine geometry: functional implication and

    regulation. *Neuron*, *46*(4), 529-532. https://doi.org/10.1016/j.neuron.2005.05.006

Hering, H., Lin, C. C., & Sheng, M. (2003). Lipid rafts in the maintenance of synapses, dendritic

    spines, and surface AMPA receptor stability. *J Neurosci*, *23*(8), 3262-3271.

    https://www.ncbi.nlm.nih.gov/pubmed/12716933

Hirano, A., & Dembitzer, H. M. (1973). Cerebellar alterations in the weaver mouse. *J Cell Biol*, *56*(2), 478-486. https://doi.org/10.1083/jcb.56.2.478

Hirano, S., & Takeichi, M. (2012). Cadherins in brain morphogenesis and wiring. *Physiol Rev*, *92*(2), 597-634. https://doi.org/10.1152/physrev.00014.2011

Holtmaat, A. J., Trachtenberg, J. T., Wilbrecht, L., Shepherd, G. M., Zhang, X., Knott, G. W., & Svoboda, K. (2005). Transient and persistent dendritic spines in the neocortex in vivo. *Neuron*, *45*(2), 279-291. https://doi.org/10.1016/j.neuron.2005.01.003

Hong, Y. K., Kim, I. J., & Sanes, J. R. (2011). Stereotyped axonal arbors of retinal ganglion cell subsets in the mouse superior colliculus. *J Comp Neurol*, *519*(9), 1691-1711. https://doi.org/10.1002/cne.22595

Horowitz, L. F., Montmayeur, J. P., Echelard, Y., & Buck, L. B. (1999). A genetic approach to trace neural circuits. *Proc Natl Acad Sci U S A*, *96*(6), 3194-3199. https://doi.org/10.1073/pnas.96.6.3194

Hoy, J. L., Bishop, H. I., & Niell, C. M. (2019). Defined Cell Types in Superior Colliculus Make Distinct Contributions to Prey Capture Behavior in the Mouse. *Curr Biol*, *29*(23), 4130-4138 e4135. https://doi.org/10.1016/j.cub.2019.10.017

Huberman, A. D., Manu, M., Koch, S. M., Susman, M. W., Lutz, A. B., Ullian, E. M., Baccus, S. A., & Barres, B. A. (2008). Architecture and activity-mediated refinement of axonal projections from a mosaic of genetically identified retinal ganglion cells. *Neuron*, *59*(3), 425-438. https://doi.org/10.1016/j.neuron.2008.07.018

Huberman, A. D., Wei, W., Elstrott, J., Stafford, B. K., Feller, M. B., & Barres, B. A. (2009). Genetic identification of an On-Off direction-selective retinal ganglion cell subtype reveals a layer-specific subcortical map of posterior motion. *Neuron*, *62*(3), 327-334. https://doi.org/10.1016/j.neuron.2009.04.014

Huntley, G. W., & Benson, D. L. (1999). Neural (N)-cadherin at developing thalamocortical synapses provides an adhesion mechanism for the formation of somatopically organized connections. *J Comp Neurol*, *407*(4), 453-471. https://www.ncbi.nlm.nih.gov/pubmed/10235639

Kay, J. N., De la Huerta, I., Kim, I. J., Zhang, Y., Yamagata, M., Chu, M. W., Meister, M., & Sanes, J. R. (2011). Retinal ganglion cells with distinct directional preferences differ in molecular identity, structure, and central projections. *J Neurosci*, *31*(21), 7753-7762. https://doi.org/10.1523/JNEUROSCI.0907-11.2011

Killen, A. C., Barber, M., Paulin, J. J. W., Ranscht, B., Parnavelas, J. G., & Andrews, W. D. (2017). Protective role of Cadherin 13 in interneuron development. *Brain Struct Funct*, *222*(8), 3567-3585. https://doi.org/10.1007/s00429-017-1418-y

Kim, I. J., Zhang, Y., Meister, M., & Sanes, J. R. (2010). Laminar restriction of retinal ganglion cell dendrites and axons: subtype-specific developmental patterns revealed with transgenic markers. *J Neurosci*, *30*(4), 1452-1462. https://doi.org/10.1523/JNEUROSCI.4779-09.2010

Kim, I. J., Zhang, Y., Yamagata, M., Meister, M., & Sanes, J. R. (2008). Molecular identification of a retinal cell type that responds to upward motion. *Nature*, *452*(7186), 478-482. https://doi.org/10.1038/nature06739

Kiser, D. P., Popp, S., Schmitt-Bohrer, A. G., Strekalova, T., van den Hove, D. L., Lesch, K. P., & Rivero, O. (2019). Early-life stress impairs developmental programming in Cadherin 13 (CDH13)-deficient mice. *Prog Neuropsychopharmacol Biol Psychiatry*, *89*, 158-168. https://doi.org/10.1016/j.pnpbp.2018.08.010

Landis, D. M., & Reese, T. S. (1977). Structure of the Purkinje cell membrane in staggerer and weaver mutant mice. *J Comp Neurol*, *171*(2), 247-260. https://doi.org/10.1002/cne.901710208

Lehto, M. T., & Sharom, F. J. (1998). Release of the glycosylphosphatidylinositol-anchored enzyme

   ecto-5'-nucleotidase by phospholipase C: catalytic activation and modulation by the lipid

   bilayer. *Biochem J*, *332 (Pt 1)*, 101-109. https://doi.org/10.1042/bj3320101

Lesch, K. P., Timmesfeld, N., Renner, T. J., Halperin, R., Roser, C., Nguyen, T. T., Craig, D. W.,

   Romanos, J., Heine, M., Meyer, J., Freitag, C., Warnke, A., Romanos, M., Schafer, H.,

   Walitza, S., Reif, A., Stephan, D. A., & Jacob, C. (2008). Molecular genetics of adult ADHD:

   converging evidence from genome-wide association and extended pedigree linkage studies. *J*

   Neural Transm (Vienna), *115*(11), 1573-1585. https://doi.org/10.1007/s00702-008-0119-3

Lien, A. D., & Scanziani, M. (2018). Cortical direction selectivity emerges at convergence of thalamic

   synapses. *Nature*, *558*(7708), 80-86. https://doi.org/10.1038/s41586-018-0148-5

Manabe, T., Togashi, H., Uchida, N., Suzuki, S. C., Hayakawa, Y., Yamamoto, M., Yoda, H.,

   Miyakawa, T., Takeichi, M., & Chisaka, O. (2000). Loss of cadherin-11 adhesion receptor

   enhances plastic changes in hippocampal synapses and modifies behavioral responses. *Mol*

   Cell Neurosci, *15*(6), 534-546. https://doi.org/10.1006/mcne.2000.0849

Matsuzaki, M., Honkura, N., Ellis-Davies, G. C., & Kasai, H. (2004). Structural basis of long-term

   potentiation in single dendritic spines. *Nature*, *429*(6993), 761-766.

   https://doi.org/10.1038/nature02617

Mavroconstanti, T., Halmoy, A., & Haavik, J. (2014). Decreased serum levels of adiponectin in adult

   attention deficit hyperactivity disorder. *Psychiatry Res*, *216*(1), 123-130.

   https://doi.org/10.1016/j.psychres.2014.01.025

May, P. J. (2006). The mammalian superior colliculus: laminar structure and connections. *Prog Brain*

   Res, *151*, 321-378. https://doi.org/10.1016/S0079-6123(05)51011-2

Miller, M., & Peters, A. (1981). Maturation of rat visual cortex. II. A combined Golgi-electron microscope study of pyramidal neurons. *J Comp Neurol*, *203*(4), 555-573. https://doi.org/10.1002/cne.902030402

Miskevich, F., Zhu, Y., Ranscht, B., & Sanes, J. R. (1998). Expression of multiple cadherins and catenins in the chick optic tectum. *Mol Cell Neurosci*, *12*(4-5), 240-255. https://doi.org/10.1006/mcne.1998.0718

Neale, B. M., Lasky-Su, J., Anney, R., Franke, B., Zhou, K., Maller, J. B., Vasquez, A. A., Asherson, P., Chen, W., Banaschewski, T., Buitelaar, J., Ebstein, R., Gill, M., Miranda, A., Oades, R. D., Roeyers, H., Rothenberger, A., Sergeant, J., Steinhausen, H. C., . . . Faraone, S. V. (2008). Genome-wide association scan of attention deficit hyperactivity disorder. *Am J Med Genet B Neuropsychiatr Genet*, *147B*(8), 1337-1344. https://doi.org/10.1002/ajmg.b.30866

Neale, B. M., Medland, S. E., Ripke, S., Asherson, P., Franke, B., Lesch, K. P., Faraone, S. V., Nguyen, T. T., Schafer, H., Holmans, P., Daly, M., Steinhausen, H. C., Freitag, C., Reif, A., Renner, T. J., Romanos, M., Romanos, J., Walitza, S., Warnke, A., . . . Psychiatric, G. C. A. S. (2010). Meta-analysis of genome-wide association studies of attention-deficit/hyperactivity disorder. *J Am Acad Child Adolesc Psychiatry*, *49*(9), 884-897. https://doi.org/10.1016/j.jaac.2010.06.008

Nguyen, P. T., Dorman, L. C., Pan, S., Vainchtein, I. D., Han, R. T., Nakao-Inoue, H., Taloma, S. E., Barron, J. J., Molofsky, A. B., Kheirbek, M. A., & Molofsky, A. V. (2020). Microglial Remodeling of the Extracellular Matrix Promotes Synapse Plasticity. *Cell*, *182*(2), 388-403 e315. https://doi.org/10.1016/j.cell.2020.05.050

Okamoto, K., Nagai, T., Miyawaki, A., & Hayashi, Y. (2004). Rapid and persistent modulation of actin dynamics regulates postsynaptic reorganization underlying bidirectional plasticity. *Nat Neurosci*, *7*(10), 1104-1112. https://doi.org/10.1038/nn1311

Perry, V. H., & Cowey, A. (1984). Retinal ganglion cells that project to the superior colliculus and

    pretectum in the macaque monkey. *Neuroscience*, *12*(4), 1125-1137.

    https://doi.org/10.1016/0306-4522(84)90007-1

Philippova, M., Ivanov, D., Joshi, M. B., Kyriakakis, E., Rupp, K., Afonyushkin, T., Bochkov, V.,

    Erne, P., & Resink, T. J. (2008). Identification of proteins associating with

    glycosylphosphatidylinositol- anchored T-cadherin on the surface of vascular endothelial

    cells: role for Grp78/BiP in T-cadherin-dependent cell survival. *Mol Cell Biol*, *28*(12), 4004-

    4017. https://doi.org/10.1128/MCB.00157-08

Poliak, S., Norovich, A. L., Yamagata, M., Sanes, J. R., & Jessell, T. M. (2016). Muscle-type Identity

    of Proprioceptors Specified by Spatially Restricted Signals from Limb Mesenchyme. *Cell*,

    164(3), 512-525. https://doi.org/10.1016/j.cell.2015.12.049

Rakic, P., & Sidman, R. L. (1973). Organization of cerebellar cortex secondary to deficit of granule

    cells in weaver mutant mice. *J Comp Neurol*, *152*(2), 133-161.

    https://doi.org/10.1002/cne.901520203

Ranscht, B., & Bronner-Fraser, M. (1991). T-cadherin expression alternates with migrating neural

    crest cells in the trunk of the avian embryo. *Development*, *111*(1), 15-22.

    https://doi.org/10.1242/dev.111.1.15

Rivero, O., Selten, M. M., Sich, S., Popp, S., Bacmeister, L., Amendola, E., Negwer, M., Schubert,

    D., Proft, F., Kiser, D., Schmitt, A. G., Gross, C., Kolk, S. M., Strekalova, T., van den Hove,

    D., Resink, T. J., Nadif Kasri, N., & Lesch, K. P. (2015). Cadherin-13, a risk gene for

    ADHD and comorbid disorders, impacts GABAergic function in hippocampus and

    cognition. *Transl Psychiatry*, *5*, e655. https://doi.org/10.1038/tp.2015.152

Rivlin-Etzion, M., Zhou, K., Wei, W., Elstrott, J., Nguyen, P. L., Barres, B. A., Huberman, A. D., &

    Feller, M. B. (2011). Transgenic mice reveal unexpected diversity of on-off direction-

selective retinal ganglion cell subtypes and brain structures involved in motion processing. *J Neurosci*, *31*(24), 8760-8769. https://doi.org/10.1523/JNEUROSCI.0564-11.2011

Rousso, D. L., Qiao, M., Kagan, R. D., Yamagata, M., Palmiter, R. D., & Sanes, J. R. (2016). Two Pairs of ON and OFF Retinal Ganglion Cells Are Defined by Intersectional Patterns of Transcription Factor Expression. *Cell Rep*, *15*(9), 1930-1944. https://doi.org/10.1016/j.celrep.2016.04.069

Ryva, B., Zhang, K., Asthana, A., Wong, D., Vicioso, Y., & Parameswaran, R. (2019). Wheat Germ Agglutinin as a Potential Therapeutic Agent for Leukemia. *Front Oncol*, *9*, 100. https://doi.org/10.3389/fonc.2019.00100

Sanders, S. J., Ercan-Sencicek, A. G., Hus, V., Luo, R., Murtha, M. T., Moreno-De-Luca, D., Chu, S. H., Moreau, M. P., Gupta, A. R., Thomson, S. A., Mason, C. E., Bilguvar, K., Celestino-Soper, P. B., Choi, M., Crawford, E. L., Davis, L., Wright, N. R., Dhodapkar, R. M., DiCola, M., . . . State, M. W. (2011). Multiple recurrent de novo CNVs, including duplications of the 7q11.23 Williams syndrome region, are strongly associated with autism. *Neuron*, *70*(5), 863-885. https://doi.org/10.1016/j.neuron.2011.05.002

Sanes, J. R., & Yamagata, M. (2009). Many paths to synaptic specificity. *Annu Rev Cell Dev Biol*, *25*, 161-195. https://doi.org/10.1146/annurev.cellbio.24.110707.175402

Shang, C., Chen, Z., Liu, A., Li, Y., Zhang, J., Qu, B., Yan, F., Zhang, Y., Liu, W., Liu, Z., Guo, X., Li, D., Wang, Y., & Cao, P. (2018). Divergent midbrain circuits orchestrate escape and freezing responses to looming stimuli in mice. *Nat Commun*, *9*(1), 1232. https://doi.org/10.1038/s41467-018-03580-7

Sibille, E., Wang, Y., Joeyen-Waldorf, J., Gaiteri, C., Surget, A., Oh, S., Belzung, C., Tseng, G. C., & Lewis, D. A. (2009). A molecular signature of depression in the amygdala. *Am J Psychiatry*, *166*(9), 1011-1024. https://doi.org/10.1176/appi.ajp.2009.08121760

Sotelo, C. (1975). Anatomical, physiological and biochemical studies of the cerebellum from mutant

   mice. II. Morphological study of cerebellar cortical neurons and circuits in the weaver

   mouse. *Brain Res*, *94*(1), 19-44. https://doi.org/10.1016/0006-8993(75)90874-4

Sotelo, C. (1990). Cerebellar synaptogenesis: what we can learn from mutant mice. *J Exp Biol*, *153*,

   225-249. https://doi.org/10.1242/jeb.153.1.225

Spranger, J., Verma, S., Gohring, I., Bobbert, T., Seifert, J., Sindler, A. L., Pfeiffer, A., Hileman, S.

   M., Tschop, M., & Banks, W. A. (2006). Adiponectin does not cross the blood-brain barrier

   but modifies cytokine expression of brain endothelial cells. *Diabetes*, *55*(1), 141-147.

   https://www.ncbi.nlm.nih.gov/pubmed/16380487

Tanaka, H., Shan, W., Phillips, G. R., Arndt, K., Bozdagi, O., Shapiro, L., Huntley, G. W., Benson,

   D. L., & Colman, D. R. (2000). Molecular modification of N-cadherin in response to

   synaptic activity. *Neuron*, *25*(1), 93-107. https://doi.org/10.1016/s0896-6273(00)80874-0

Tang, L., Hung, C. P., & Schuman, E. M. (1998). A role for the cadherin family of cell adhesion

   molecules in hippocampal long-term potentiation. *Neuron*, *20*(6), 1165-1175.

   https://doi.org/10.1016/s0896-6273(00)80497-3

Tanihara, H., Sano, K., Heimark, R. L., St John, T., & Suzuki, S. (1994). Cloning of five human

   cadherins clarifies characteristic features of cadherin extracellular domain and provides

   further evidence for two structurally different types of cadherin. *Cell Adhes Commun*, *2*(1), 15-

   26. https://doi.org/10.3109/15419069409014199

Tantra, M., Guo, L., Kim, J., Zainolabidin, N., Eulenburg, V., Augustine, G. J., & Chen, A. I. (2018).

   Conditional deletion of Cadherin 13 perturbs Golgi cells and disrupts social and cognitive

   behaviors. *Genes Brain Behav*, *17*(6), e12466. https://doi.org/10.1111/gbb.12466

Terracciano, A., Sanna, S., Uda, M., Deiana, B., Usala, G., Busonero, F., Maschio, A., Scally, M.,

   Patriciu, N., Chen, W. M., Distel, M. A., Slagboom, E. P., Boomsma, D. I., Villafuerte, S.,

Sliwerska, E., Burmeister, M., Amin, N., Janssens, A. C., van Duijn, C. M., . . . Costa, P. T., Jr. (2010). Genome-wide association scan for five major dimensions of personality. *Mol Psychiatry*, *15*(6), 647-656. https://doi.org/10.1038/mp.2008.113

Tiihonen, J., Rautiainen, M. R., Ollila, H. M., Repo-Tiihonen, E., Virkkunen, M., Palotie, A., Pietilainen, O., Kristiansson, K., Joukamaa, M., Lauerma, H., Saarela, J., Tyni, S., Vartiainen, H., Paananen, J., Goldman, D., & Paunio, T. (2015). Genetic background of extreme violent behavior. *Mol Psychiatry*, *20*(6), 786-792. https://doi.org/10.1038/mp.2014.130

Tonnesen, J., Katona, G., Rozsa, B., & Nagerl, U. V. (2014). Spine neck plasticity regulates compartmentalization of synapses. *Nat Neurosci*, *17*(5), 678-685. https://doi.org/10.1038/nn.3682

Treutlein, J., Cichon, S., Ridinger, M., Wodarz, N., Soyka, M., Zill, P., Maier, W., Moessner, R., Gaebel, W., Dahmen, N., Fehr, C., Scherbaum, N., Steffens, M., Ludwig, K. U., Frank, J., Wichmann, H. E., Schreiber, S., Dragano, N., Sommer, W. H., . . . Rietschel, M. (2009). Genome-wide association study of alcohol dependence. *Arch Gen Psychiatry*, *66*(7), 773-784. https://doi.org/10.1001/archgenpsychiatry.2009.83

Tsai, N. Y., Wang, F., Toma, K., Yin, C., Takatoh, J., Pai, E. L., Wu, K., Matcham, A. C., Yin, L., Dang, E. J., Marciano, D. K., Rubenstein, J. L., Wang, F., Ullian, E. M., & Duan, X. (2022). Trans-Seq maps a selective mammalian retinotectal synapse instructed by Nephronectin. *Nat Neurosci*, *25*(5), 659-674. https://doi.org/10.1038/s41593-022-01068-8

Tsukamoto, Y., & Omi, N. (2017). Classification of Mouse Retinal Bipolar Cells: Type-Specific Connectivity with Special Reference to Rod-Driven AII Amacrine Pathways. *Front Neuroanat*, *11*, 92. https://doi.org/10.3389/fnana.2017.00092

Uchida, N., Honjo, Y., Johnson, K. R., Wheelock, M. J., & Takeichi, M. (1996). The catenin/cadherin adhesion system is localized in synaptic junctions bordering transmitter release zones. *J Cell Biol*, *135*(3), 767-779. https://doi.org/10.1083/jcb.135.3.767

Uhl, G. R., Drgon, T., Johnson, C., Li, C. Y., Contoreggi, C., Hess, J., Naiman, D., & Liu, Q. R. (2008). Molecular genetics of addiction and related heritable phenotypes: genome-wide association approaches identify "connectivity constellation" and drug target genes with pleiotropic effects. *Ann N Y Acad Sci*, *1141*, 318-381. https://doi.org/10.1196/annals.1441.018

Vaughn, J. E. (1989). Fine structure of synaptogenesis in the vertebrate central nervous system. *Synapse*, *3*(3), 255-285. https://doi.org/10.1002/syn.890030312

Vaughn, J. E., Henrikson, C. K., & Grieshaber, J. A. (1974). A quantitative study of synapses on motor neuron dendritic growth cones in developing mouse spinal cord. *J Cell Biol*, *60*(3), 664-672. https://doi.org/10.1083/jcb.60.3.664

Vestal, D. J., & Ranscht, B. (1992). Glycosyl phosphatidylinositol--anchored T-cadherin mediates calcium-dependent, homophilic cell adhesion. *J Cell Biol*, *119*(2), 451-461. https://doi.org/10.1083/jcb.119.2.451

Walker, C. K., Greathouse, K. M., Boros, B. D., Poovey, E. H., Clearman, K. R., Ramdas, R., Muhammad, H. M., & Herskowitz, J. H. (2021). Dendritic Spine Remodeling and Synaptic Tau Levels in PS19 Tauopathy Mice. *Neuroscience*, *455*, 195-211. https://doi.org/10.1016/j.neuroscience.2020.12.006

Xu, W., Cohen-Woods, S., Chen, Q., Noor, A., Knight, J., Hosang, G., Parikh, S. V., De Luca, V., Tozzi, F., Muglia, P., Forte, J., McQuillin, A., Hu, P., Gurling, H. M., Kennedy, J. L., McGuffin, P., Farmer, A., Strauss, J., & Vincent, J. B. (2014). Genome-wide association study of bipolar disorder in Canadian and UK populations corroborates disease loci

including SYNE1 and CSMD1. *BMC Med Genet*, *15*, 2. https://doi.org/10.1186/1471-2350-15-2

Yamagata, M., Herman, J. P., & Sanes, J. R. (1995). Lamina-specific expression of adhesion molecules in developing chick optic tectum. *J Neurosci*, *15*(6), 4556-4571. https://www.ncbi.nlm.nih.gov/pubmed/7790923

Yamagata, M., Sanes, J. R., & Weiner, J. A. (2003). Synaptic adhesion molecules. *Curr Opin Cell Biol*, *15*(5), 621-632. https://doi.org/10.1016/s0955-0674(03)00107-8

Yang, J., Wang, S., Yang, Z., Hodgkinson, C. A., Iarikova, P., Ma, J. Z., Payne, T. J., Goldman, D., & Li, M. D. (2015). The contribution of rare and common variants in 30 genes to risk nicotine dependence. *Mol Psychiatry*, *20*(11), 1467-1478. https://doi.org/10.1038/mp.2014.156

Yogev, S., & Shen, K. (2014). Cellular and molecular mechanisms of synaptic specificity. *Annu Rev Cell Dev Biol*, *30*, 417-437. https://doi.org/10.1146/annurev-cellbio-100913-012953

Yoshihara, Y., Mizuno, T., Nakahira, M., Kawasaki, M., Watanabe, Y., Kagamiyama, H., Jishage, K., Ueda, O., Suzuki, H., Tabuchi, K., Sawamoto, K., Okano, H., Noda, T., & Mori, K. (1999). A genetic approach to visualization of multisynaptic neural pathways using plant lectin transgene. *Neuron*, *22*(1), 33-41. https://doi.org/10.1016/s0896-6273(00)80676-5

Zhang, Y., Kim, I. J., Sanes, J. R., & Meister, M. (2012). The most numerous ganglion cell type of the mouse retina is a selective feature detector. *Proc Natl Acad Sci U S A*, *109*(36), E2391-2398. https://doi.org/10.1073/pnas.1211547109

Zhou, K., Dempfle, A., Arcos-Burgos, M., Bakker, S. C., Banaschewski, T., Biederman, J., Buitelaar, J., Castellanos, F. X., Doyle, A., Ebstein, R. P., Ekholm, J., Forabosco, P., Franke, B., Freitag, C., Friedel, S., Gill, M., Hebebrand, J., Hinney, A., Jacob, C., . . . Asherson, P. (2008). Meta-analysis of genome-wide linkage scans of attention deficit hyperactivity

disorder. *Am J Med Genet B Neuropsychiatr Genet*, *147B*(8), 1392-1398.

https://doi.org/10.1002/ajmg.b.30878

Ziv, N. E., & Smith, S. J. (1996). Evidence for a role of dendritic filopodia in synaptogenesis and

spine formation. *Neuron*, *17*(1), 91-102. https://doi.org/10.1016/s0896-6273(00)80283-4

Publishing Agreement

It is the policy of the University to encourage open access and broad distribution of all theses, dissertations, and manuscripts. The Graduate Division will facilitate the distribution of UCSF theses, dissertations, and manuscripts to the UCSF Library for open access and distribution. UCSF will make such theses, dissertations, and manuscripts accessible to the public and will take reasonable steps to preserve these works in perpetuity.

I hereby grant the non-exclusive, perpetual right to The Regents of the University of California to reproduce, publicly display, distribute, preserve, and publish copies of my thesis, dissertation, or manuscript in any form or media, now existing or later derived, including access online for teaching, research, and public service purposes.

DocuSigned by:

Angela Matcham

50689302C8A047C...   Author Signature

12/13/2022

Date